DEGREE PROJECT

Thin layer of particles during deep penetration laser dispersing

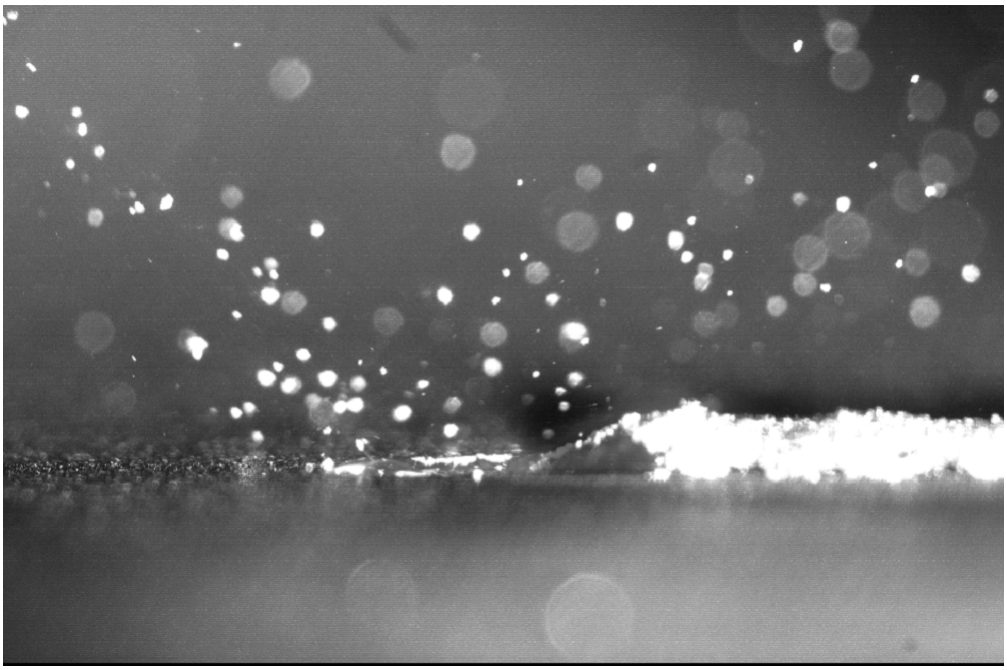

Javier De La Llana Pablos

Mechanical Engineering, bachelor's level
2019

Luleå University of Technology
Department of Engineering Sciences and Mathematics

LULEÅ UNIVERSITY OF TECHNOLOGY

Acknowledgements

This thesis has been possible thanks to the support of many people. I would like to thank all members of the Product and Production Development Division for their support during these months. I would also like to thank my examiner, Jörg, and my supervisor, Adrien, for their help and advice during all the process to make this project come to fruition.

- Javier De La Llana Pablos -

Abstract

This report aims at gaining a better understanding of the conditions that enable the formation of a micro-clad layer of powder on top of the melt pool during a laser deep penetration dispersing process, using the work of previous projects as a starting point. Two different powder materials, TiN and TiC, were tested on two different substrates, stainless steel and zinc coated steel. The influence of some process parameters such as the laser speed, the position of the powder nozzle (in front or on the back of the laser) and the distance between the nozzle and the keyhole were be studied as well.

Samples from the previous year project were studied beforehand in order to define new parameters to investigate through other experiments.

The obtained samples were analysed with an optical microscope, as well as with a stereo microscope and a SEM.

The obtained tracks were compared together in order to find out the influence of the corresponding parameters on the powder particles dispersion in the melt pool.

For some combinations of parameters, a micro-clad layer of about 50 to 100 µm was formed on the surface of the melt pool.

Finally, some suggestions for future work regarding this topic were proposed.

Abstract (SE)

Denna rapport syftar till att få en bättre förståelse av de förhållanden som möjliggör bildandet av ett mikroklättat lager av pulver ovanpå smältbassängen under en laser-djup penetreringsdispersionsprocess, med utgångspunkt från tidigare projekters arbete. Två olika pulvermaterial, TiN och TiC, testades på två olika substrat, rostfritt stål och zinkbelagt stål. Påverkan av vissa processparametrar, såsom laserns hastighet, läget för pulvermunstycket (framåt eller på laserens baksida) och avståndet mellan munstycket och nyckelhålet studerades också.

Prover från föregående års projekt studerades i förväg för att definiera nya parametrar för att undersöka genom andra experiment. De erhållna proven analyserades med ett optiskt mikroskop, såväl som med ett stereomikroskop och en SEM.

De erhållna spåren jämfördes tillsammans för att ta reda på påverkan av motsvarande parametrar på dispersionen av pulverpartiklar i smältpoolen.

För vissa kombinationer av parametrar bildades ett mikroklädt skikt av omkring 50 till 100 µm på ytan av smältpoolen.

Slutligen föreslogs några förslag till framtida arbete angående detta ämne.

Contents

1. Introduction

1.1. Background

Cladding of surfaces using laser is a well-known process used in order to improve some properties of a certain material, such as the wear resistance or corrosion resistance. This is achieved through the addition of powder of a different material with the wished properties after heating the area with laser, creating a layer over the base material.

It has been found in previous experiments that it is also possible to form a much thinner micro-clad layer with a process of deep penetration dispersing, where the powder particles remain on top of the keyhole melt pool. However, the conditions that enable this thin layer to form are not fully understood yet.

1.1.1. Motivation

The aim of this project is to investigate further into the conditions that allow the formation of the micro-clad layer, exploring the influence of variables that have not been considered in previous experiment, as well as the influence the materials have in this phenomenon.

1.2. Aim

A better understanding of the formation of this layer would allow to improve the properties of the base material, while reducing the amount of powder used in the process as no powder would penetrate the melt pool.

1.3. Methodology

For this purpose, the development of this study will be divided into several phases:

- Literature study: further research into the previous experiments, as well as into papers related with this topic in order to elaborate a state-of-the-art to proportionate this study a theoretical basis

- Analysis of previous samples: the study of the unanalysed samples from the last experiment, in case they can proportionate some information of interest.

- Establishment of new parameters: deciding which parameters of the new experiments with the information provided by the state-of-the-art and the findings in the analysis of the previous samples.

- New experiments: will be carried out in the laser laboratory, following the parameters previously established.

- New samples analysis: finally, the resulting tracks of the new experiments will be analysed and compared, in order to reach a conclusion on this topic.

2. Theory

This section will cover the theoretical research and state-of-the-art of the project, which will later be used as a base for the discussion of the results.

2.1. Laser dispersing

Laser dispersing is a process which objective is to distribute powder particles into a melt pool on the base material, in order to improve its properties.

For this process, the substrate is first melted with the laser. Depending on the input power, this can be done whether in heat conduction regime (more shallow but wider melt pool), or in keyhole regime (more narrow and deeper melt pool). The condition for each regime to happen is the input power of the laser, around 1 MW/cm^2. Above this threshold, the keyhole regime will occur. Below 100 kW/cm^2, conduction regime will happen. Between both values a transition zone exists.

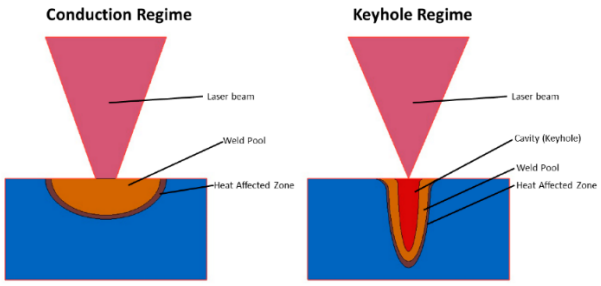

Fig. 1. *Dispersing regimes*

While the laser is acting, a stream of powder particles of a material which the wished characteristics, blown into the substrate by one or more nozzles, will penetrate the melt pool.

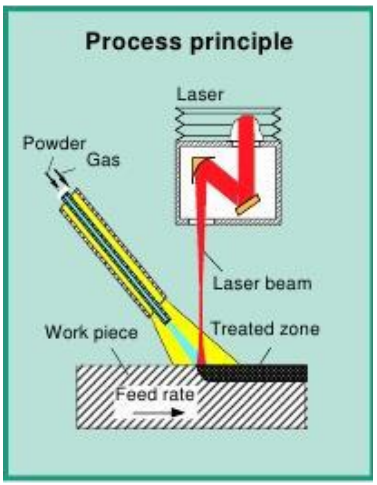

Fig. 2. *Laser dispersing*

This process is used to achieve a homogenous improvement along the cross section of the material, rather than only in the surface.

2.2. Laser Cladding

The process of laser cladding consists on forming a layer of a certain material over the surface of another material, known as substrate or base material. The main difference from the process of laser dispersing is that in this case the base material is not melted. Laser cladding is used to improve some of the surface properties, such as its wear or corrosion resistance, as well as increasing the hardness.

For this method, the laser scans a track over the substrate, heating it. Then, the metallic powder is added by injecting it through one of several nozzles over the heat affected area. The powder particles will then melt and attach to the surface, forming a layer on top of it.

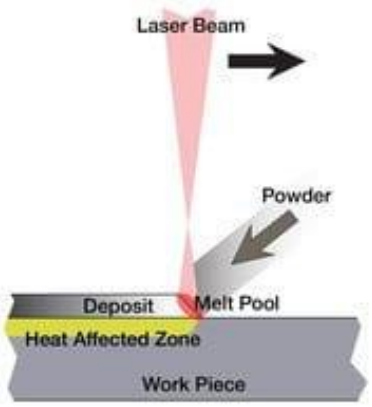

Fig. 3. *Laser cladding*

2.3. Particle behaviour inside the melt pool

There are several material properties that affect the distribution and penetration of the particles, such as surface tension and viscosity. A high surface tension and viscosity have shown to support the powder movement within the pool (1), while on the other hand, lower surface tension and viscosity seem to benefit the particle incorporation in the melt pool. (2) The higher surface tension tends to occur in the sides of the melt pool, while the centre presents a lower one. In other words, this means that a powder particle will be less prone to penetrate inside in the central zone, and the clad layer will be more likely to form in the sides.

Moreover, a particle must be heated up enough before being able to incorporate into the melt pool, generally by absorbing the energy from the laser beam. If a particle happens to absorb enough energy to partly melt its surface, the entry into the melt pool is improved. (2) (3)

Therefore, depending on both the substrate and the base, it will be easier for the powder to penetrate the melt pool, or instead remain on its surface. This is because heat absorptivity and surface tension play an important role on the behaviour of the behaviour of the particle inside the melt pool.

Another condition for the particle to enter the melt pool is that the particles must have enough kinetic energy to overcome the surface tension of the melt.

The kinetic energy depends on several parameters: the velocity of the particle (vp), the mass (mp) and the inclination angle of the nozzle (φ), with the following relation (3):

$$E_{kin} = \frac{1}{2} m_p \cdot (v_p * \sin(\varphi))^2$$

The minimum speed a particle needs to enter the melt pool is calculated with the expression (3):

$$v_{min} = \sqrt{\frac{3}{2 \cdot \rho \cdot \gamma_{lv} \cdot d}} \cdot (\gamma_{lv} + \gamma_{lp} - \gamma_{pv})$$

With d being the diameter of the particle (assuming a spherical particle shape), γ_{lv} being the surface tension between the liquid and the vapour, γ_{lp} the surface tension between liquid and particle, and γ_{pv} the surface tension between particle and vapor. These values depend on the materials, and on the contact angle between liquid and vapor, with the following relation (3):

$$\gamma_{lp} = \gamma_{pv} - \gamma_{lv} \cdot \cos(\Theta)$$

In research regarding the method of laser sintering, it was found that the sintered density (amount of powder particles per unit of area) depended on both the powder type and the process parameters, with density increasing as laser power increases and scan velocity decreases. A higher density means a lower layer thickness with the same scane line spacing. Other factors that affect the density are: the atmosphere, as an argon atmosphere seems to give better densification that a nitrogen atmosphere, although the different is not too significant; and the presence of oxygen, as the formation of an oxide layer on the surface of powder particles improves the absorption rate of laser radiation. (4)

The setup of the experiment can also help in the distribution of the powder materials.

For instance, coaxial nozzles are usually preferable to an independent powder nozzle, as higher angles are possible. This helps the particles to penetrate the melt pool. Also, their stability is superior to that of the independent nozzles, so the accuracy and number of particles that interact with the track will also increase. (5)

It is also worth noting that, in cladding operations at very high particle temperatures and speeds, the particle can detach from the substrate, as the heat exchange is not fast enough to solidify them. (5)

2.4. Impact of materials

The selection of materials for both the base material and the powder materials has an impact on the final distribution of the powder through the cross section and their chances of penetrating inside or remaining on the surface.

Some properties of the powder that benefit the assimilation of the powder into the melt pool are a low melting temperature, low thermal conductivity and high absorptivity of the laser energy (5). For example, a high absorptivity and low melting temperature can cause the surface of the particles to melt before contacting with the substrate. This means that a liquid surface will come into contact with another liquid surface, instead of having a solid on liquid wetting contact, therefore improving the particle entry into the melt pool. (3)

The following table is a comparison between the thermal properties of the different materials that are part of this study (3) (6):

Material	**Density (g/cm^3)**	**Melting temperature (ºC)**	**Thermal conductivity (W/mK)**	**Thermal capacity (J/(mol·K))**
TiN	5.22	2930	19.2 – 56.8	37.2
TiC	4.92	3140	17.1 – 30.9	34.1
WC-Co	15.6	2850	28 – 88	54.8
TiB_2	4.52	3230	24 – 58	46.5
B_4C	2.52	2763	30 – 42	50.9
Steel (substrate)	7.75 – 8.05	1300 – 1400	20 – 50	28
Zinc (coating)	7.14	420	116	25.5

Table 1. *Thermal properties of materials*

In the WC-Co powder mixture, the WC is the structural powder, while Co is the binder (which has a lower melting point to make the assimilation into the melt pool faster) (7). In previous experiments, particles of WC-Co are not significantly affected by fluid flow, being more prone to stay on the upper part of the cross section, but they show a more irregular distribution in width. In some cases, they stay on the centre of the cross section, while in others they accumulate at the sides. (1)

On the other hand, TiB_2 powder particles seemed to have a more homogeneous distribution in the melt pool. (1)

Moreover, WC-Co particles showed less material removal during wear tests than if using TiB_2 powder, as well as a higher wear resistance in the base material. The reason of this behaviour is likely to be the change on the particle transport mechanism caused by the different combinations of powder and base materials. For example, the TiB2 particles, having a lower density, are more likely to be transported throughout the cross section. (1)

B_4C particles seem to accumulate in the upper regions of the cross section, and they seem to maintain this behaviour when using different modulation strategies, and their low density means they are not likely to sink in the melt pool, unlike WC-Co (which has a higher density). (3)

On the other hand, WC-Co powder is more appropriate to be processed under a wide range of parameters, unlike other powder mixtures such as Fe-Cu, due to its high absorption ad low reflectivity, as well as the unequal characteristics between WC and Co powders. (8)

Aside from the thermal properties, another factor that determines the particle distribution in the melt pool is, as explained in the previous paragraph, the surface tension of the material. This property influences the minimum velocity a particle must have in order to penetrate the melt pool (3). Moreover, the possible chemical reactions that may occur are also important for the capacity of assimilation of the particles into the melt pool. For example, in WC-Co powder, the Co is oxidized during the process, reducing the assimilation of powder into the pool. (3)

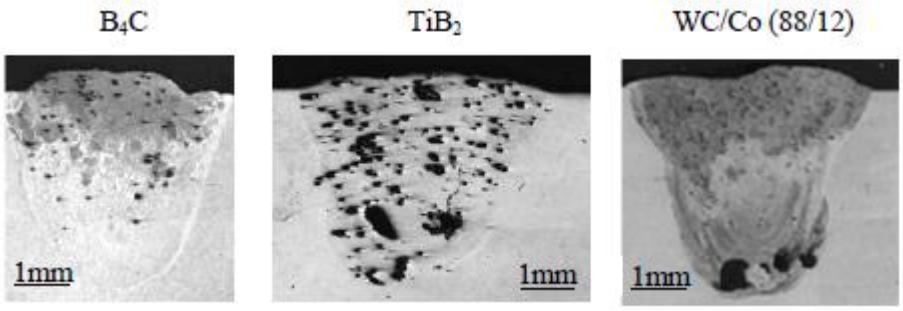

Fig. 4. *Difference in particle distribution (3)*

According to (1), the combination of materials is the most important factor for the particle distribution, even more than the different operation parameters.

2.5. Impact of parameters

Some parameters for the laser process that have been studied in the literature and should be considered for this study are the following ones:

- Laser power: in general, a higher energy input leads to the formation of a wider and deeper melt pool forming a bigger keyhole and making the particle assimilation easier. This is because in the vicinity of the surface, the high temperatures cause the melt to be oxide free and with a low surface tension. In order to achieve a deep penetration welding the power input must be above the energy threshold (generally, around 1 MW/cm^3). Otherwise, a heat conduction welding will occur in its place. However, the homogeneity of the particle distribution in the cross section is not significantly affected by this parameter, as the welding depth is increased as well. (1)

- Laser velocity: if the powder flow rate is constant, a lower laser velocity will cause more particles to enter the melt pool. At high speeds, the track width is reduced, but the transport of particles in depth is improved. (1)

- Powder mass flow: depends on both the rotation speed of the feeding plate, and the volumetric gas flow. A higher gas pressure, theoretically, was expected to cause more particles to enter the melt pool, as their speed, and therefore their kinetic energy, will increase. However, this has not been reflected in the experiments, although it has shown a tendency of distributing particles deeper than with lower pressures. On the other hand, an increase in the powder feed rate with the same gas flow leads to higher amounts of particles present in the melt pool, although it does not have a significant impact on their distribution. (1)

2.6. Previous experiments results

In the experiments carried during the Laser Material Processing course during the last two years, the obtained results were:

- In the 2017 project (*Homogeneity of TiC particles distribution during laser deep dispersing*), TiC powder particles were used with a Hardox 450 steel as base material, with several attempts varying the laser velocity and the gas flow. Some of the results of this experiment showed an unexpected clad layer of powder material on the upper part of the weld, which is the phenomenon to study in the current project. (9)

- In the 2018 project (*Thin layer of particles during deep penetration laser dispersing*), two different powder particles were used: TiN and TiC, over two base materials: stainless steel and zinc coated steel, varying several parameters such as process velocity and powder velocity. Several samples were studied, although in any of them a complete homogeneous clad layer was formed. It was found that the zinc coated presented a more consistent clad layer (although also more porosity) than the stainless steel. Moreover, a decreased powder transporting gas flow and decreased process velocity seemed to benefit the formation of the clad layer. The fact that a

decreased powder transporting gas flow leads to a better clad layer is thought to be due to the instability of the process and the geometry of the nozzles. A more accurate nozzle, such a coaxial one, is expected to give a more homogeneous distribution of the particles. (10)

3. Analysis of previous samples

In the experiment carried during the last Laser material processing course, which studied the same phenomenon as in this project, the micro clad layer, there were several parameters that were not analysed. The objective of the following paragraph is to study those previous samples to see if they can give some new information that can be useful for this project.

3.1. Process parameters

Out of the 12 samples that were obtained in last experiment, only numbers 1 to 5 and number 11 were studied. In this report, the rest of them (6-10 and 12) will be prepared for their analysis.

The processing parameters that were for the mentioned samples were:

Fiber diameter	0.4 mm
Focusing lens	250 mm
Collimating lens	150 mm
Beam diameter	0.67 mm
Angle of the nozzle	40-45º
Plate rotation speed	2 rpm
Laser power	3 kW
Mass flow rate (TiN)	6.8 g/min
Particle size (TiN)	-90+45 µm

Table 2. *Constant process parameters*

Sample	Powder	Laser velocity (m/min)	Gas flow (l/min)	Base material
6	TiN	3	6	Stainless steel
7	TiN	3	8	Stainless steel
8	TiN	3	4	Stainless steel
9	TiN	2	4	Stainless steel
10	TiN	4	4	Stainless steel
12	TiN	3	4	Zinc coated steel

Table 3. *Variable process parameters*

3.2. Sample preparation

In order to prepare the samples for observations, different processing steps were required.

First, they were cut with a cutting wheel for ferrous metals across the middle section of the track, which will be the studied cross section. Then, they were cold mounted in phenolic powder. Afterwards, they were grinded and polished in several steps. Finally, they were etched around 5 seconds each with 3% Nital Acid, in order to improve the visibility of the microsctructure in each part of the cross section more easily.

3.3. Sample observation

To observe the cross section, an optical microscope with an incorporated camera was used. Pictures of two different magnifications, 2.5 and 10, were taken.

Furthermore, a SEM (Scanning Electron Microscope) was performed in sample 6, in order to determine the composition of several parts of the cross section.

In the following section, each of the pictures will be presented, with a brief discussion about them.

Sample 6

TiN on Stainless steel; Laser velocity = 3 m/min; Gas flow = 6 l/min

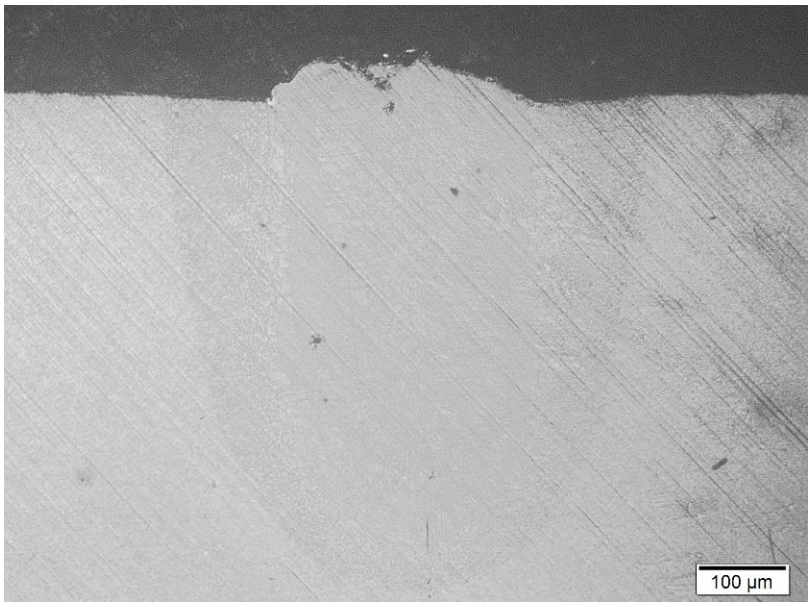

Fig. 5. *Sample 6 x2.5*

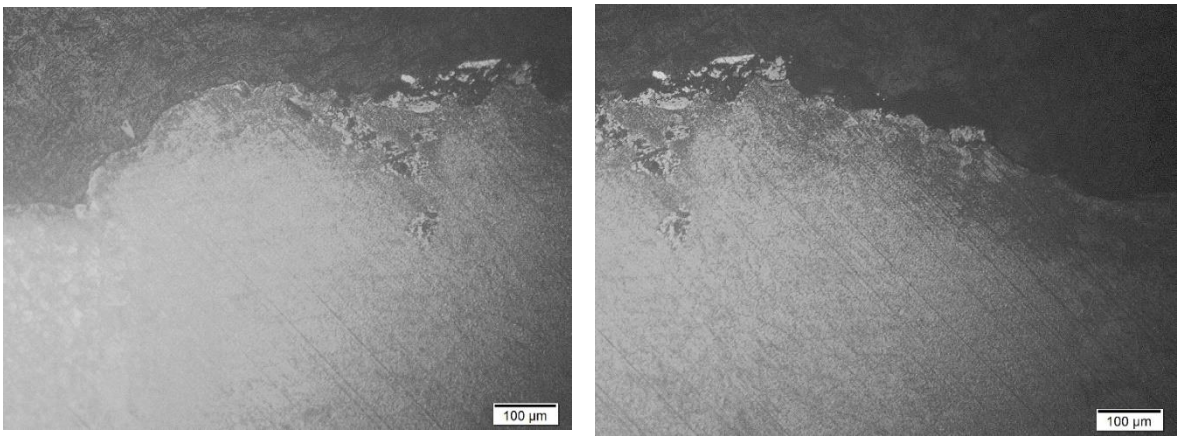

Fig. 6. *Sample 6 x10*

The EDS in the following points of the cross section:

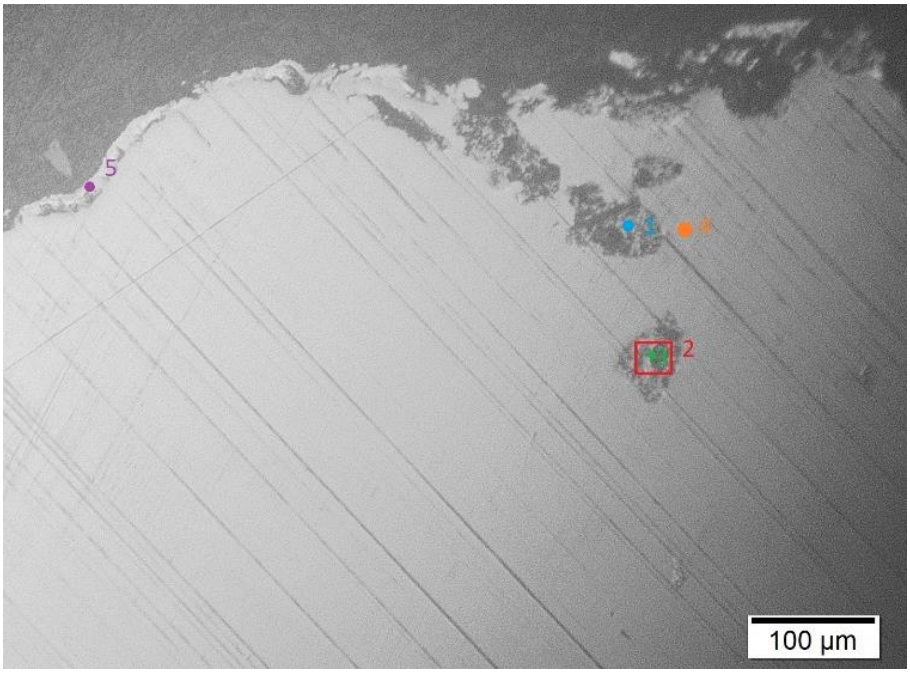

***Fig. 7**. Sample 6 Points for EDS analysis*

Giving the following results:

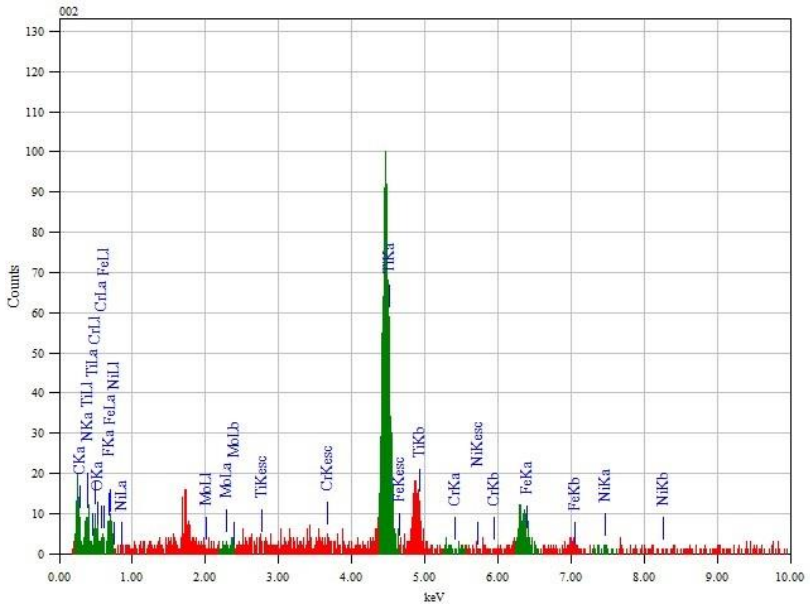

***Fig. 8.** EDS point 1*

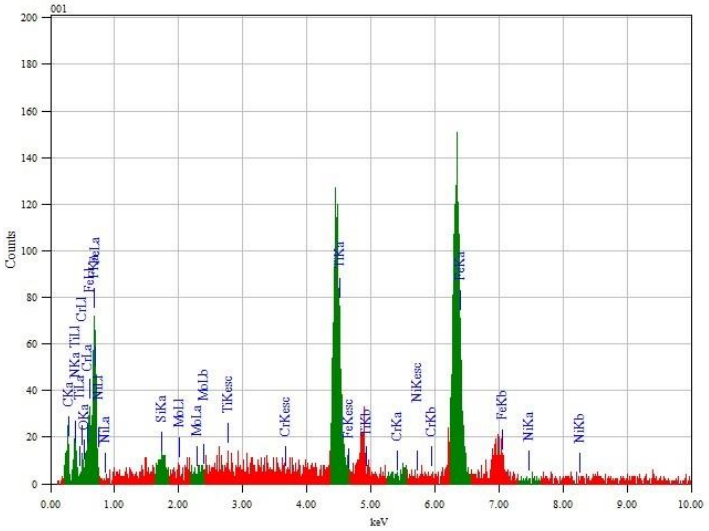

Fig. 9. *EDS area 2*

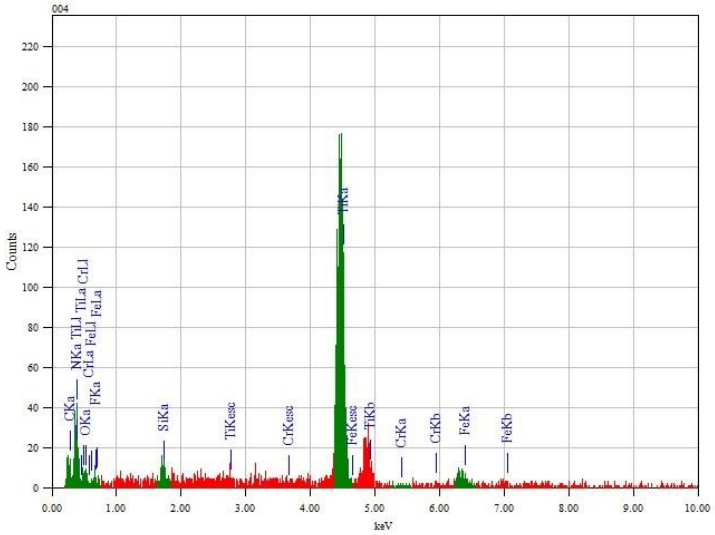

Fig. 10. *EDS point 3*

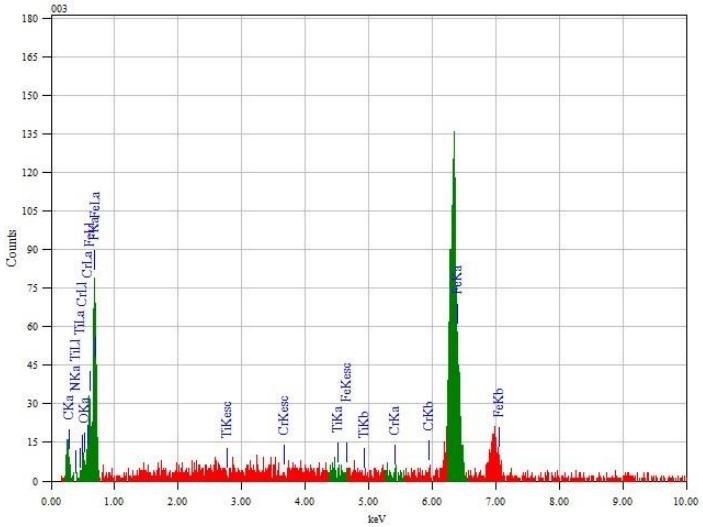

Fig. 11. *EDS point 4*

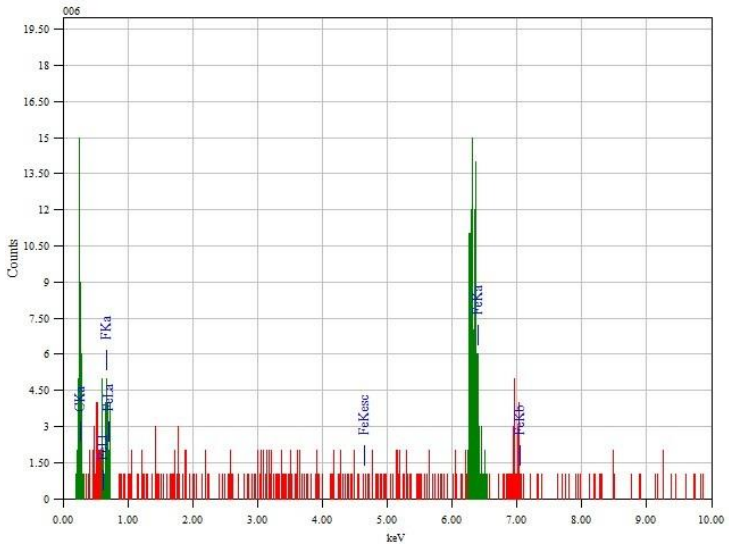

***Fig. 12**. EDS point 5*

It can be concluded from the results that the darker spots are TiN particles, while the lighter ones correspond to the base material (stainless steel).

In these images, it can be seen that the wished clad layer has not been formed on top of the melt pool. Although there are some particles present in the centre of the top of the track, a high fraction of the powder has penetrated the melt pool instead of remaining on top of it. Furthermore, there are no particles at the sides.

Sample 7

TiN on Stainless steel; Laser velocity = 3 m/min; Gas flow = 8 l/min

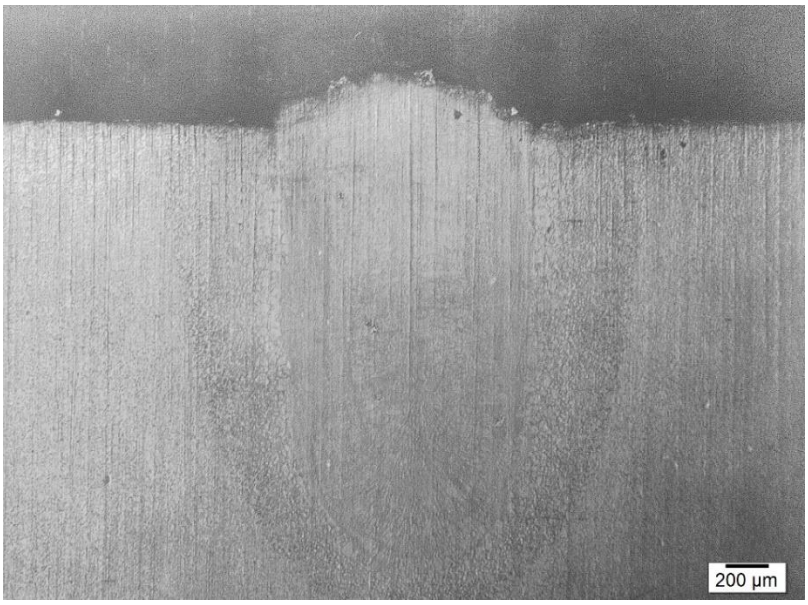

Fig. 13. *Sample 7 x2.5*

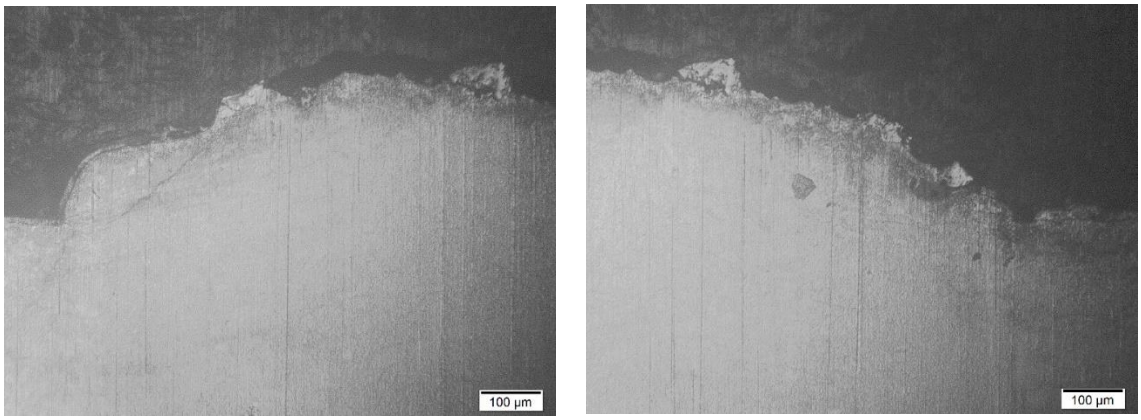

Fig. 14. *Sample 7 x10*

In this case, no powder has penetrated the melt pool. However, the amount of powder present is less than in the previous case, and only a few particles are present at the top of the melt pool.

Sample 8

TiN on Stainless steel; Laser velocity = 3 m/min; Gas flow = 4 l/min

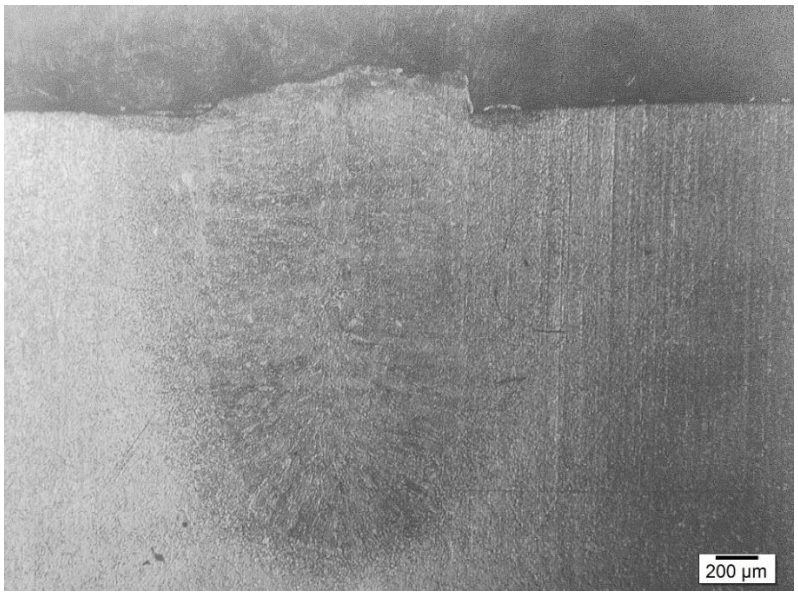

Fig. 15. *Sample 8 x2.5*

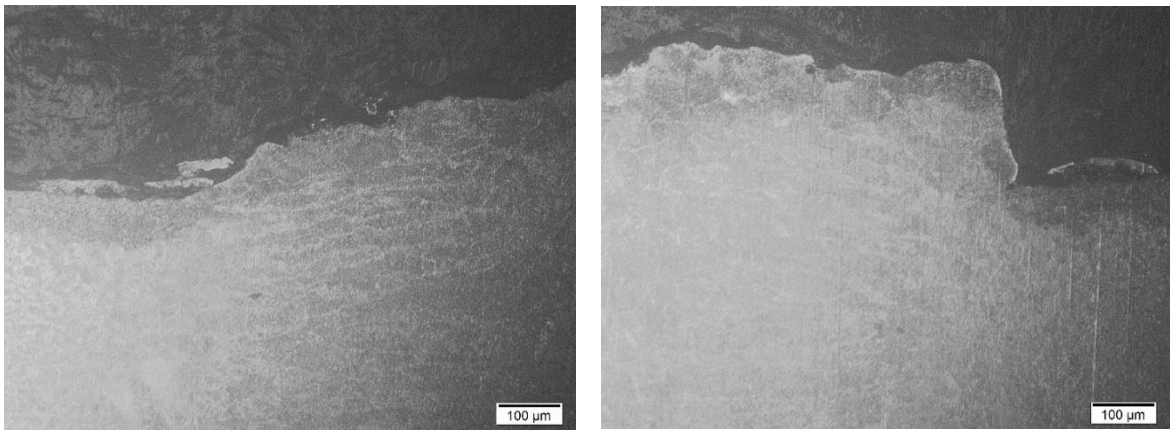

Fig. 16. *Sample 8 x10*

In this sample, there are not visible particles at the top of the melt pool. On the other hand, there is no penetration of powder inside it.

Sample 9

TiN on Stainless steel; Laser velocity = 2 m/min; Gas flow = 4 l/min

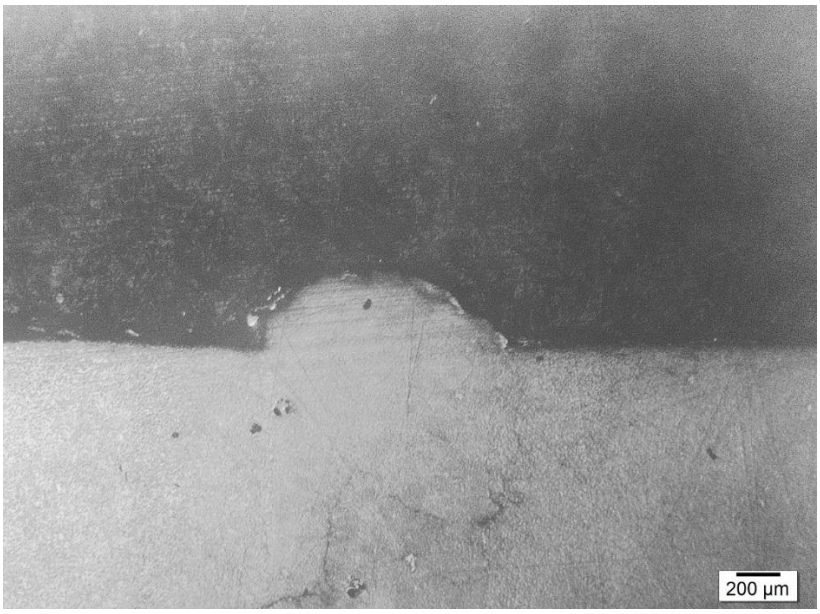

Fig. 17. *Sample 9 x2.5*

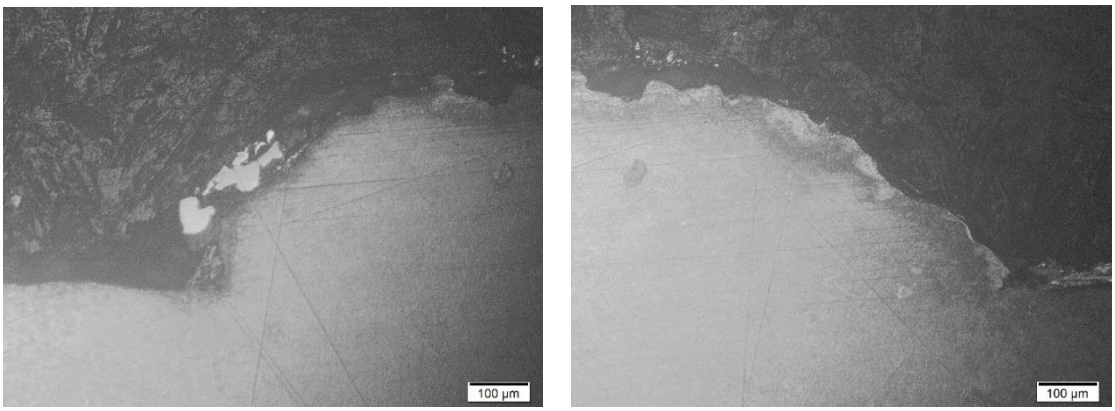

Fig. 18. *Sample 9 x10*

In this case, a few particles can be observed at the top. There is also a small quantity of powder into the melt pool.

Sample 10

TiN on Stainless steel; Laser velocity = 4 m/min; Gas flow = 4 l/min

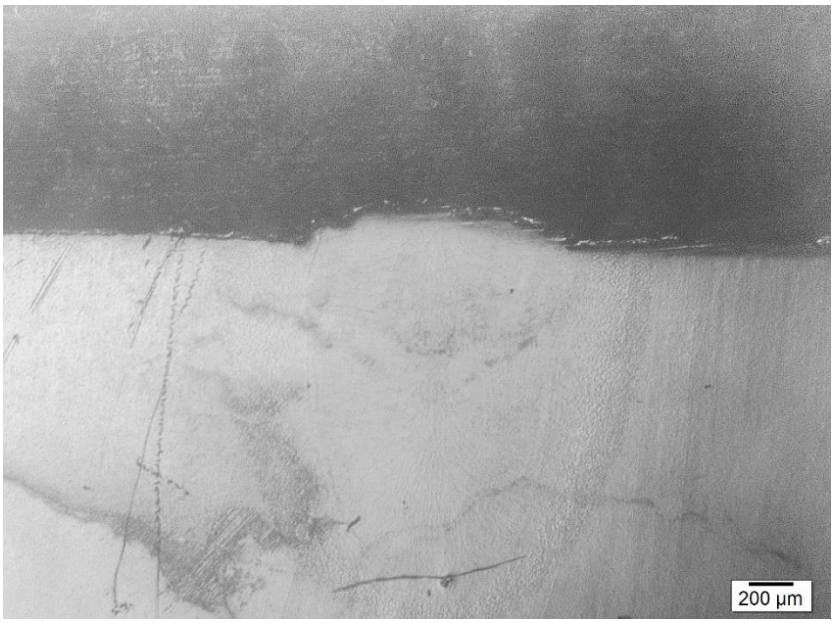

Fig. 19. *Sample 10 x2.5*

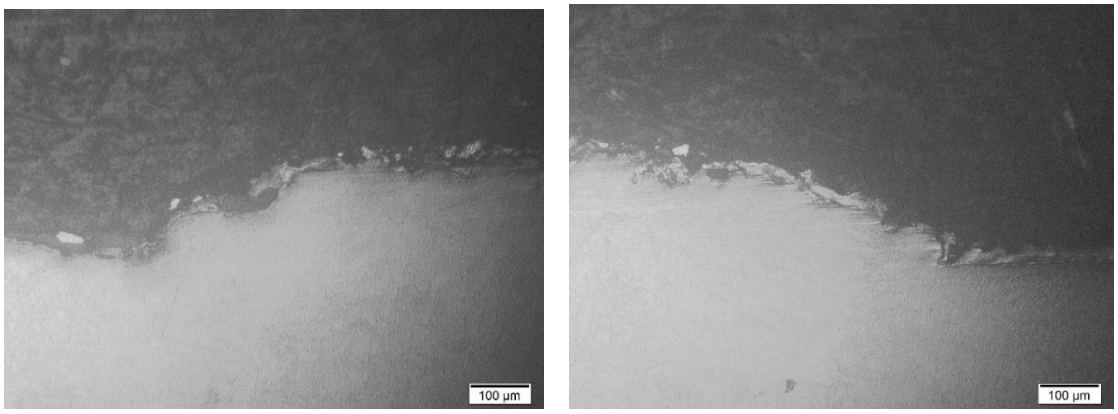

Fig. 20. *Sample 10 x10*

A low number of molten particles can be seen in the central part of the top surface. Furthermore, there are no particles inside the melt pool.

Sample 12

TiN on Zinc coated steel; Laser velocity = 3 m/min; Gas flow = 4 l/min

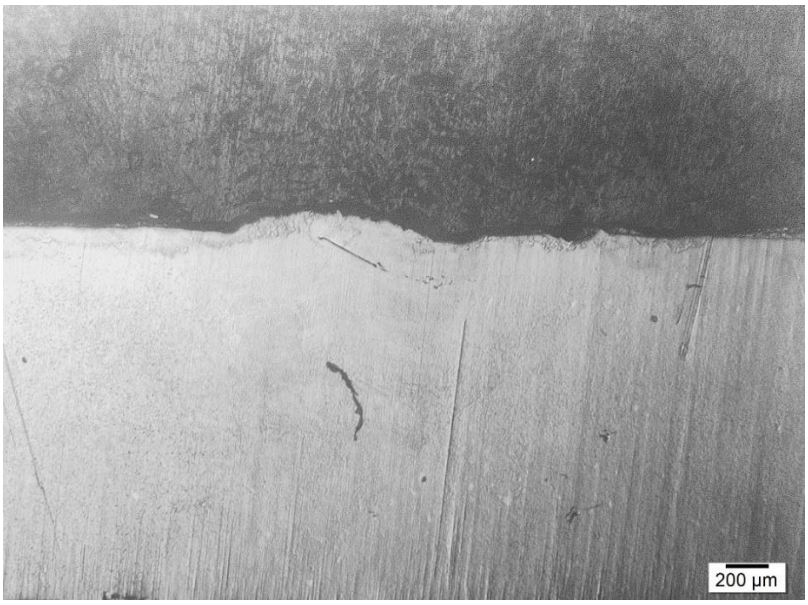

Fig. 21. *Sample 12 x2.5*

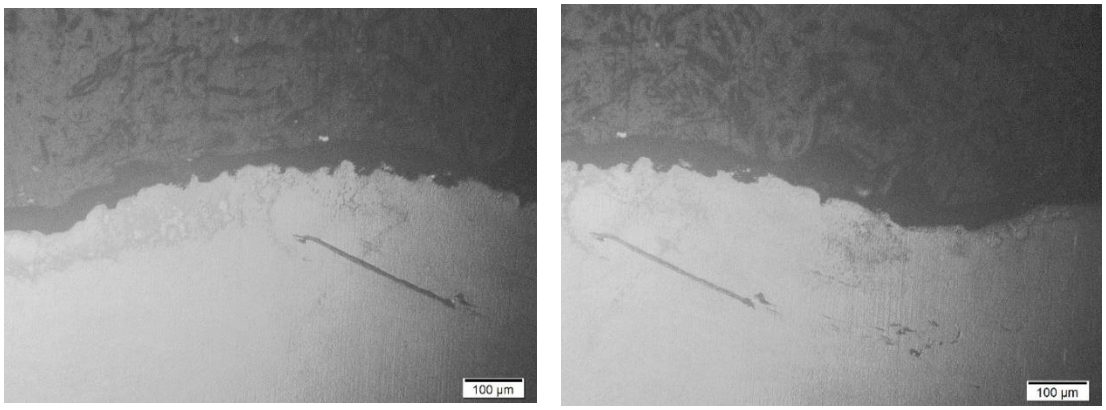

Fig. 22. *Sample 12 x10*

In this case, practically no particles can be seen in the entire cross section.

3.4. Discussion

After analysing the pictures, several comparisons between the samples can be made, considering the variation of parameters that occurred between them.

Comparing samples 6, 7 and 8, a correlation between the gas flow rate and the distribution of the powder particles in the cross section can be established. It can be seen that this parameter does not affect in a significant way the amount of powder present in the cross section. However, an increase on the gas flow affects the distribution of particles in it, with more powder penetrating the melt pool than with lower flow rates.

Comparing samples 8, 9 and 10, which experimented a variation of laser speed between them, the laser speed does not seem to have a great influence on the amount of powder in this case, as all of them present a very low number of particles.

It also can be seen that, comparing to the results obtained in the previous experiment of samples 1 to 5, the TiN powder generally presents a slightly lower level of dispersion into the melt pool than the TiC powder, although given the similar density of these two materials, the difference is not very significant.

Finally, track 12 (which was performed with the same parameters as track 8, changing base material from stainless steel to zinc coated steel) does not present many differences from number 8,

It can be concluded that the main problem that can be seen is that the amount of powder present in all the cross sections is very low, so a clad layer could not be formed due to the lack of material.

Therefore, the focus for the following experiments should be studying which parameters can increase the amount of powder particles present in the melt pool.

4. New experiments

This section will cover the methodology followed for the new experiments in the laser laboratory, as well as the experimental plan and parameters decided for them.

4.1. Variation of parameters

As seen in the analysis of the previous samples, the main problem is the low number of particles present in the melt pool. Therefore, the decision of the parameters will be focused on this matter.

The parameters that have been considered are:

- **Nozzle angle and distance:** in order to prevent the particles from bouncing on the surface, the angle of the nozzle should be high. Due to the limitations of placement of the nozzle in the laser bench, a realistic high laser angle would be around 50º, versus the 45º angle that was used in the previous experiments. Furthermore, the influence of the placement and distance from the nozzle to the melt pool will be studied as well. Instead of doing all the experiments with the powder nozzle placed behind the laser, most of them will be performed with it in front of the laser, trying as well different distance between the extreme of the nozzle and the keyhole.

- **Materials:** according to the literature (1), WC-Co powder showed a tendency of staying in top of the melt pool, so it was considered as a possible powder material for the experiment. However, this was not possible due to its small size (-24 + 5 µm), which would cause it to be stuck in the feeding machine. Therefore, TiN and TiC powder were kept as the powder materials, as well as the substrate materials still being Stainless steel and Zinc Coated Steel.

- **Laser speed:** slower speeds have shown to let more particles to interact with the melt pool (1), so speeds in the range of 2 and 3 m will be tested.

- **Powder mass flow rate:** this parameter must be increased in order to have more powder in the melt pool. It can be changed in two ways: by modifying the rotational speed of the feed table, or by varying the gas flow rate. A high gas flow rate interacted with the melt pool in such a way that the particles were not assimilated into the melt pool, rather causing an effect similar to remote cutting, so it will be kept at a relatively low level (4 l/min). Therefore, the solution for this problem is to increase the rotational speed of the feeding table instead. The mass rate in the previous experiments was 6.8 g/min, so in these new experiments it will be increased to 10 g/min.

4.2. Experimental plan

After these considerations, the final experimental plan was:

Fiber diameter	0.4 mm
Focusing lens	250 mm
Collimating lens	150 mm
Beam diameter	0.67 mm
Angle of the nozzle	52º
Nozzle distance from keyhole	X: 6 mm (+ position); Y: 6 mm
Table rotation speed	2.75 rpm
Mass flow rate	10 g/min
Particle size (TiN)	-90+45 µm
Particle size (TiC)	-90+45 µm

Table 4. *Constant experiment parameters*

Sample	Nozzle side	Nozzle position	Powder material	Base material	Laser speed (m/min)	Gas flow rate (l/min)
1*	Front	keyhole	TiN	Stainless steel	3	17
1.2	Front	keyhole	TiN	Stainless steel	3	4
2	Front	1 mm	TiN	Stainless steel	3	4
3	Front	2 mm	TiN	Stainless steel	3	4
4*	Back	keyhole	TiN	Stainless steel	3	17
5*	Back	1 mm	TiN	Stainless steel	3	17
5.2	Back	1 mm	TiN	Stainless steel	3	4
6	Back	2 mm	TiN	Stainless steel	3	4
7	Front	keyhole	TiN	Zinc coated steel	3	4
8	Front	keyhole	TiC	Zinc coated steel	3	4
9	Front	keyhole	TiN	Stainless steel	1	4
10	Front	keyhole	TiC	Stainless steel	3	4
11	Front	keyhole	TiN	Stainless steel	2	4
12	Front	keyhole	TiN	Zinc coated steel	2	4
13	Back	keyhole	TiC	Stainless steel	3	4

Table 5. *Variable experiment parameters*

***Note:** Samples 1, 4 and 5 were performed with a gas flow of 17 l/min due to errors during calibration. The rest of the experiments, including 1.2 and 5.2, were performed with the expected gas flow rate of 4 l/min.

4.3. Experiment methodology

The experiment was conducted in the laser laboratory, using an Yb:YAG fiber laser which incorporated a 3d movement table in order to place the samples.

The setup is shown in the following schematic:

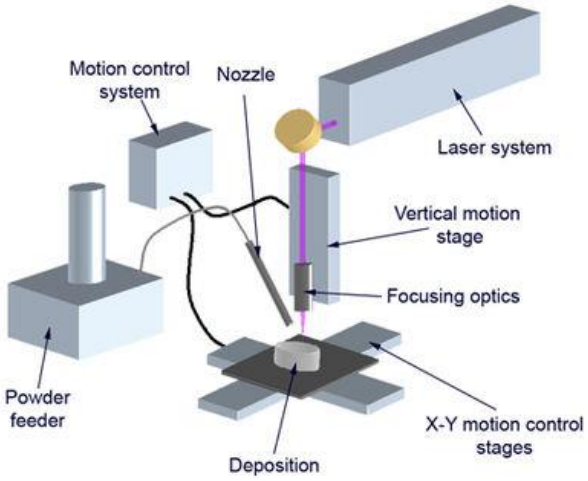

Fig. 23. *Schematic of experiment*

Additionally, a HIS (High speed imaging) system was installed to film the laser process, in order to visualize the flow of the melt pool and the behaviour of the particles after coming into contact with the substrate.

In order to get the necessary table rotation speed to achieve a powder mass flow of 10 g/min, some tests were made before the experiment, with several speeds, by blowing the powder into a recipient.

In 30 seconds, the following results were obtained:

Mass of powder blown in 30 seconds (g)	**Table rotational speed (rpm)**
1.4	1
2.3	1.5

Table 6. *Powder mass flow*

Establishing a correlation, the necessary rotational speed for 10 g/min was estimated to be around 2.75 rpm.

The following pictures show the real setup of the experiments. The HSI camera, powder nozzle placement and powder feeding table can be seen:

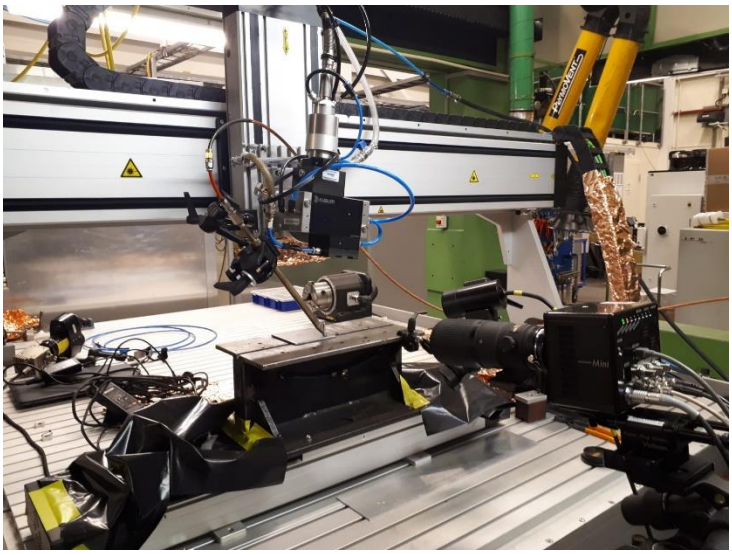

Fig. 24. *Experiment setup*

Fig. 25. *Powder feeding table*

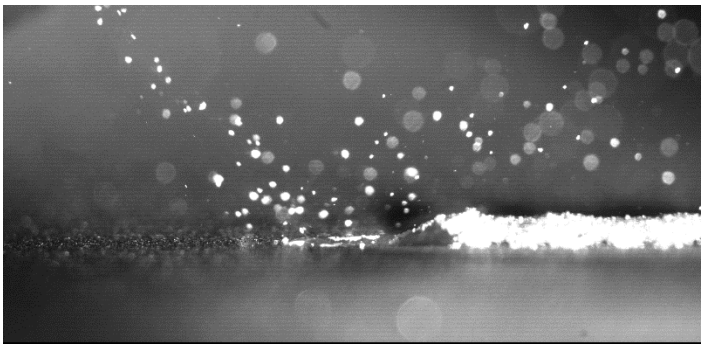

Fig. 26. *High Speed Imaging*

5. Analysis of new samples

This section will cover the study of the results from the new experiments, as well as a brief discussion about each of the obtained tracks.

5.1. Sample preparation

The next step after finalizing the experiment is to prepare the samples for their observation and study, in a similar way as the previous ones.

The aspect of the different tracks after the process was as the following images show:

Fig. 27. *Resulting tracks*

The three tracks marked as 0 are not part of the experiment, as they were used to test the High Speed Imaging (HSI) camera.

Moreover, it can also be appreciated that four of the tracks (3, 4, 5 and 5.2) exhibited an irregular distribution of powder along the track, with parts of it where the clad layer accumulated, and parts where there is no molten material, so they were not studied in this report.

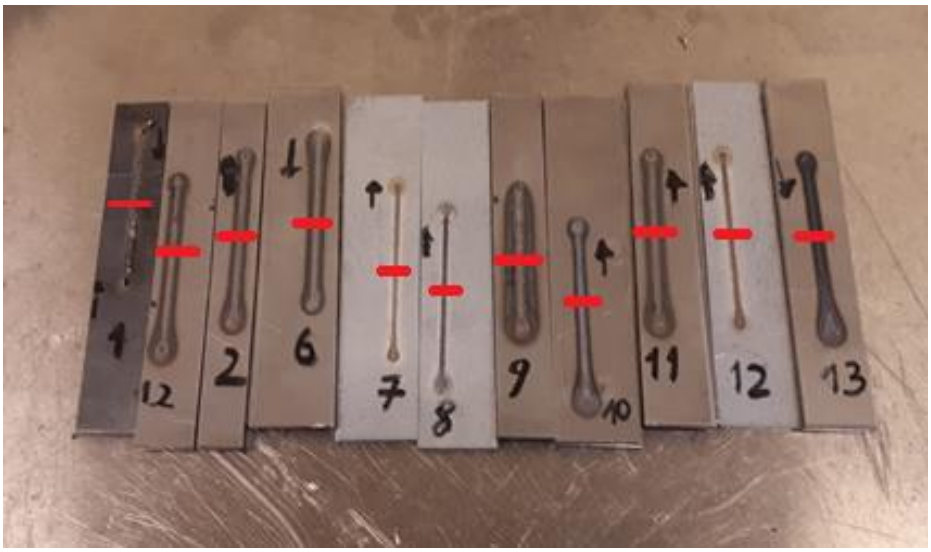

Fig. 28. *Studied tracks with cuts*

For the observation, they were prepared in the Sample preparation room, in a similar way to the previous samples.

5.2. Sample observation

To study the tracks, the middle cross section was first observed through an optical microscope with an incorporated camera. Pictures were taken with two magnifications, x2.5 and x10. After observing the pictures, some samples showed some structures that were worth to be further looked into.

For this purpose, three of the tracks (7, 11 and 12) were subject of an EDS analysis using a SEM for this purpose

Additionally, all the tracks were observed through a stereo microscope, both the cross section and the upper surface, as the colour of the image showed the composition of each part in a more clear way.

In the following section, all the pictures for each sample will be presented, as well as the EDS results and a brief discussion about each of them.

Sample 1

TiN on Stainless steel; Front side; keyhole position; laser velocity = 3 m/min; Gas flow rate =17 l/min

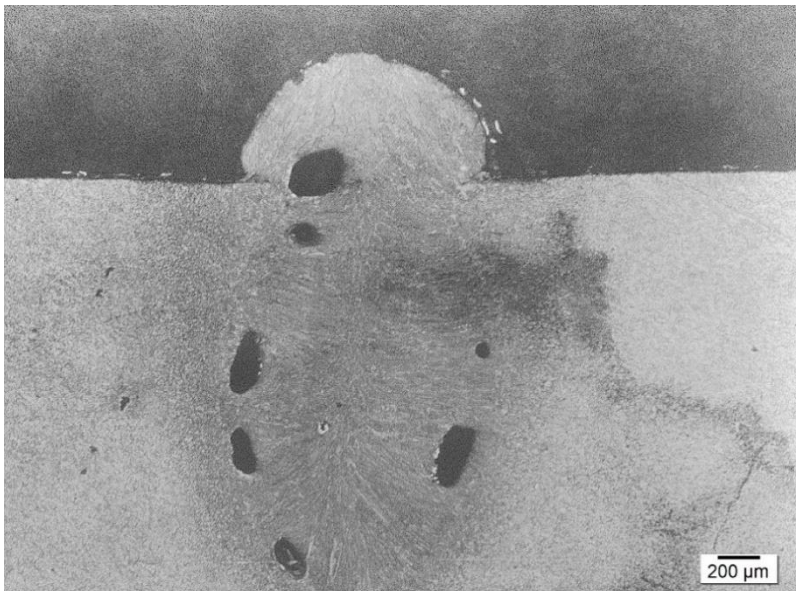

Fig. 29. *Sample 1 x2.5*

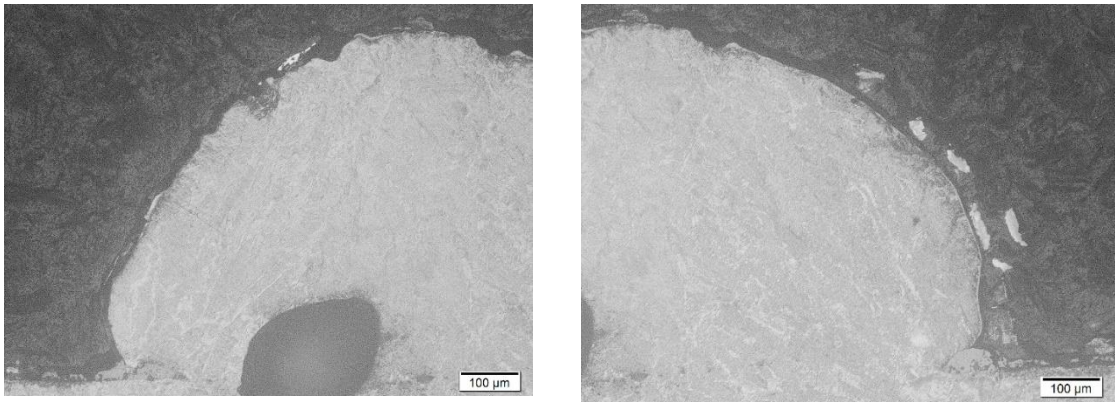

Fig. 30. *Sample 1 x10*

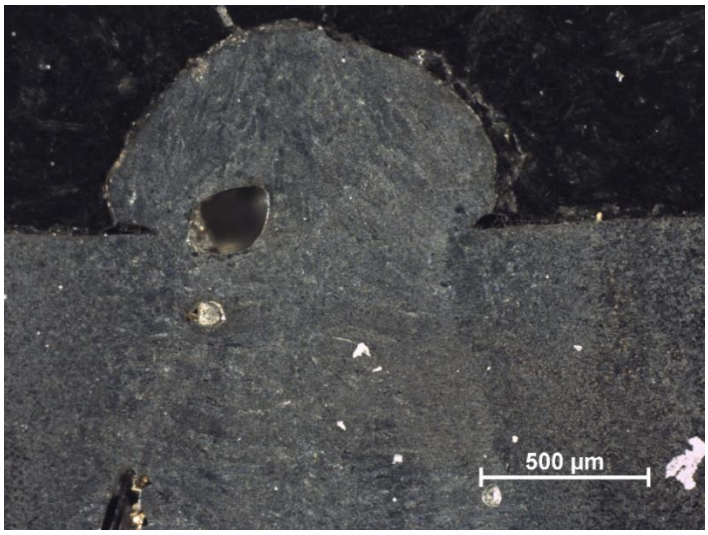

Fig. 31. *Sample 1 Cross section recorded by a stereo microscope*

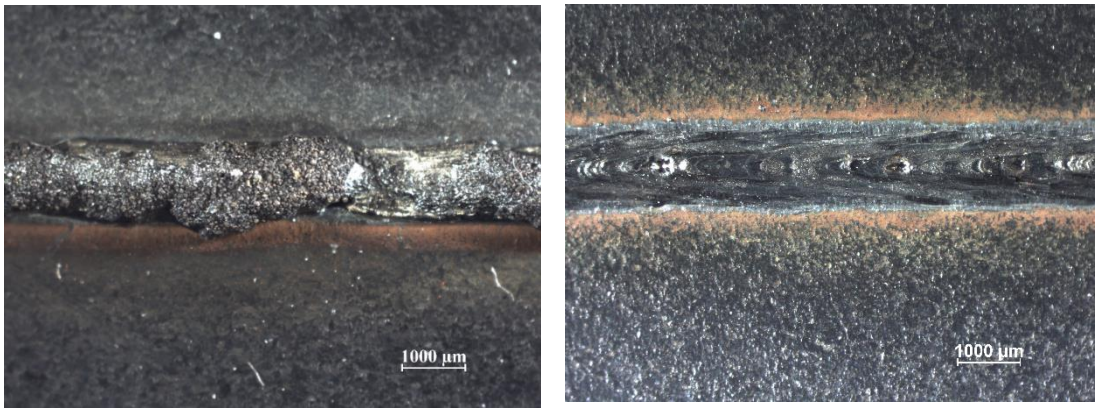

Fig. 32. *Sample 1 top surface recorded by a stereo microscope and example of a track with no powder*

In this sample, there is not a consistent clad layer over the melt pool. Some noticeable aspects of this sample are the elevated height of the melt pool – result of the flow during the laser process –, the big size of the pores present on the inside, and the fact that the powder does not seem to be equally distributed along the track, which is likely caused by the flow of the melt pool.

Additionally, an example of a track performed with no powder on it and with the same process parameters and substrate as sample 1 can be seen by the top surface image taken by the stereo microscope. The differences are noticeable. Particularly, the influence of the transporting gas on the flow of the melt can be seen.

Sample 1.2

TiN on Stainless steel; Front side; keyhole position; laser velocity = 3 m/min; Gas flow rate =4 l/min

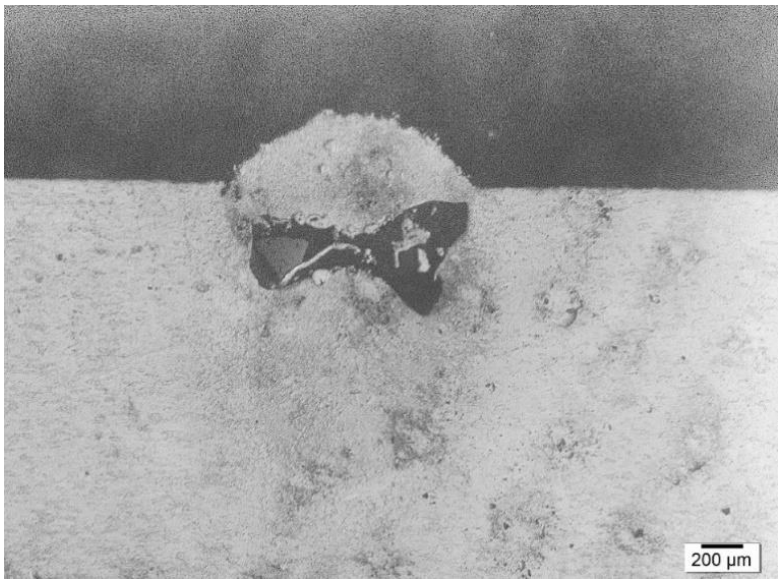

Fig. 33. *Sample 1.2 x2.5*

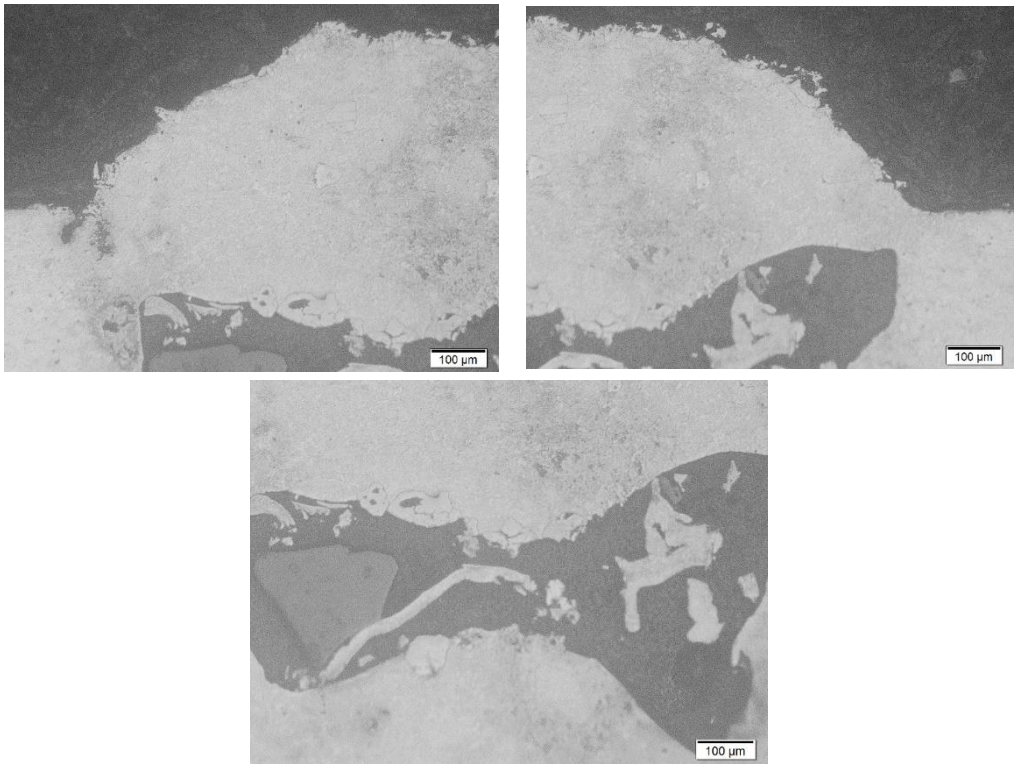

Fig. 34. *Sample 1.2 x10*

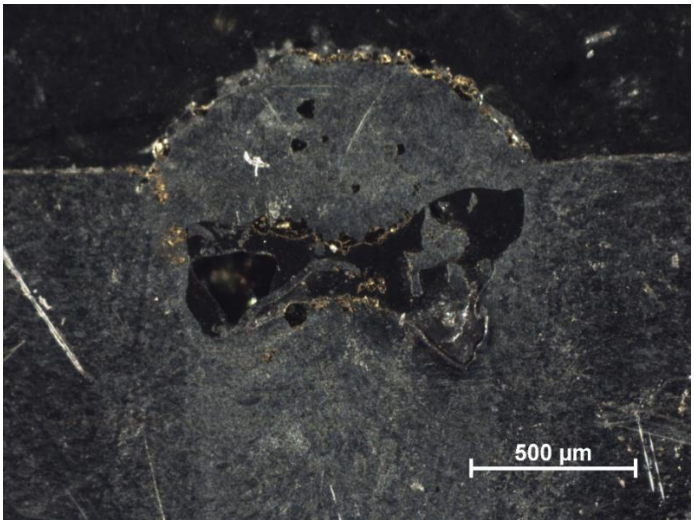

Fig. 35. *Sample 1.2 Cross section recorded by a stereo microscope*

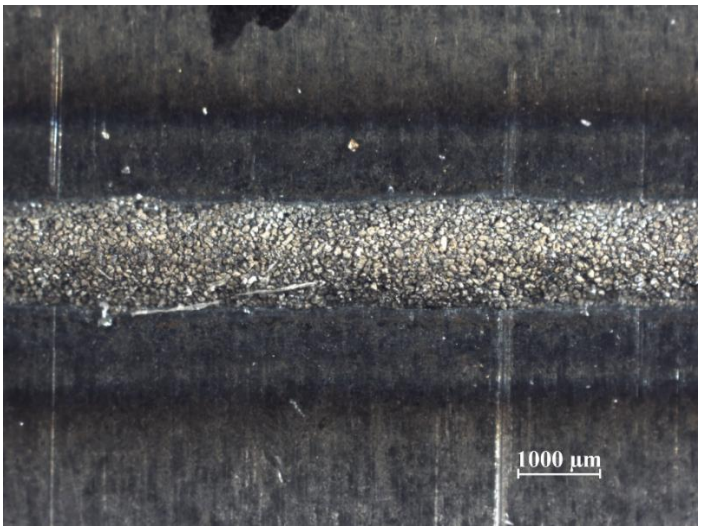

Fig. 36. *Sample 1.2 top surface recorded by a stereo microscope*

In this case, a thin clad layer appears to have formed, with the thickness of the powder particles (50 µm). It also shows an equal distribution of the powder along the track. However, there is a huge pore inside the melt pool, with some powder around it. The presence of this pore is detrimental for the performance of the surface, as it represents a weak point in the material.

Sample 2

TiN on Stainless steel; Front side; 1 mm from keyhole; laser velocity = 3 m/min; Gas flow rate = 4 l/min

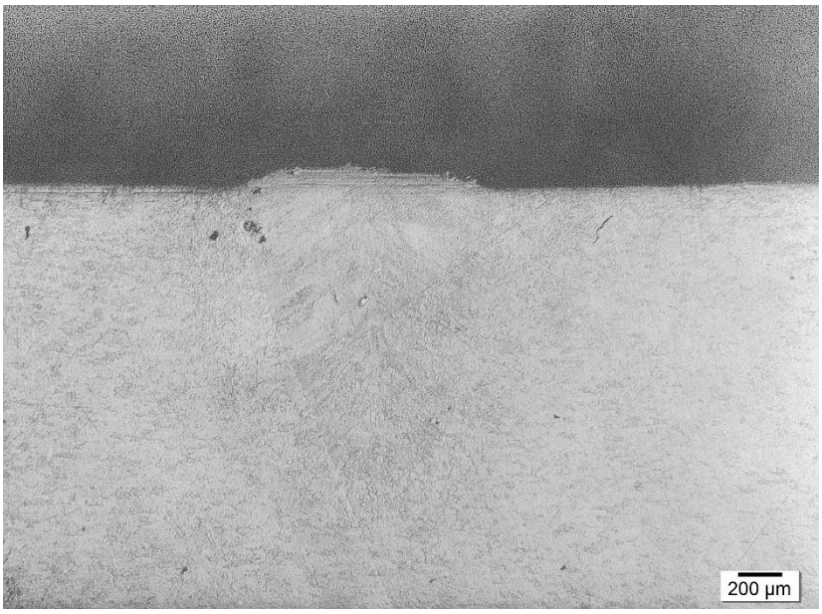

Fig. 37. *Sample 2 x2.5*

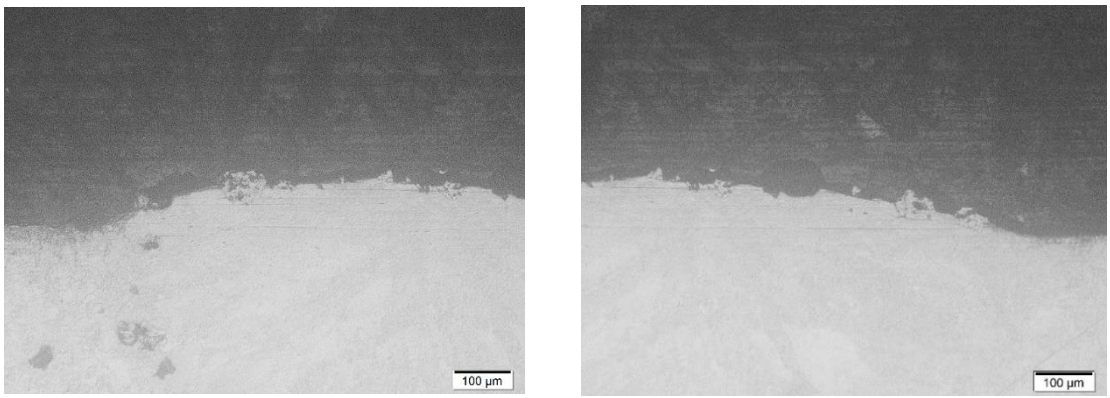

Fig. 38. *Sample 2 x10*

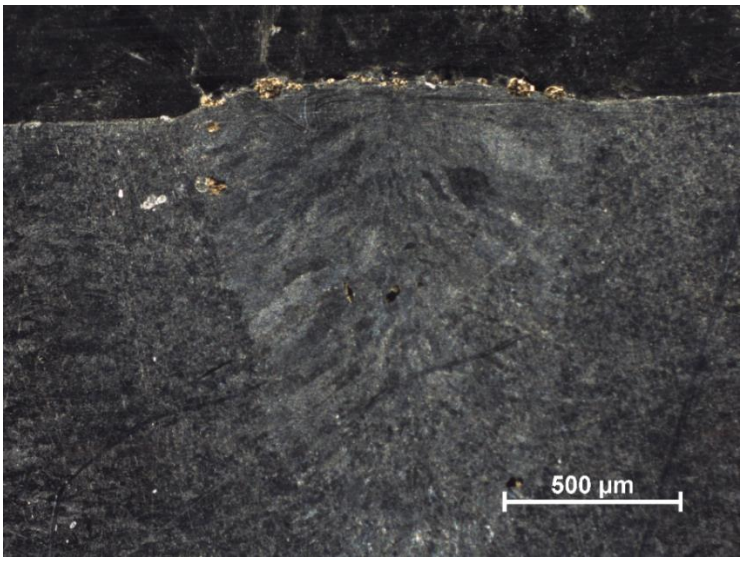

Fig. 39. *Sample 2 Cross section recorded by a stereo microscope*

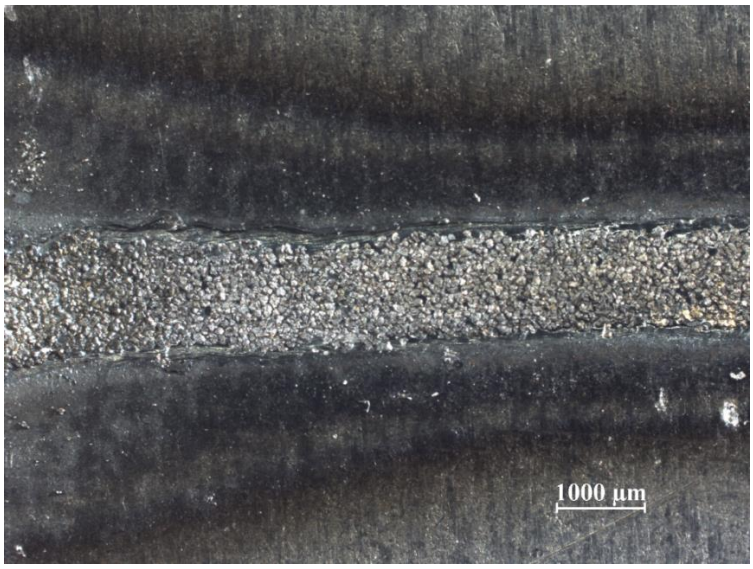

Fig. 40. *Sample 2 top surface recorded by a stereo microscope*

A partial clad layer with a thickness of about 50 µm appears to be present in this sample, with some clear areas with no powder. Moreover, there is almost no dispersion of powder inside the melt pool, and it is equally distributed along the track.

Sample 6

TiN on Stainless steel; Back side; 2 mm from keyhole; laser velocity = 3 m/min; Gas flow rate = 4 l/min

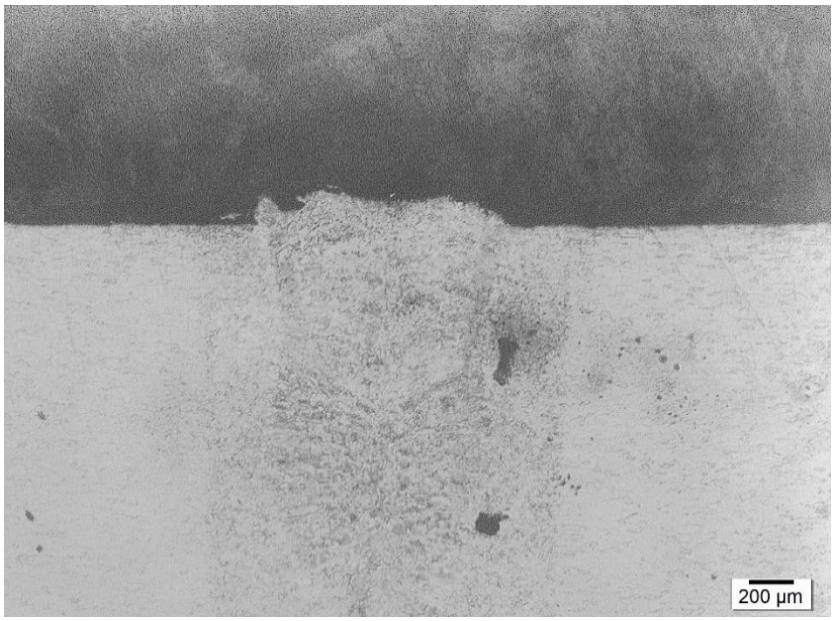

Fig. 41. *Sample 6 x2.5*

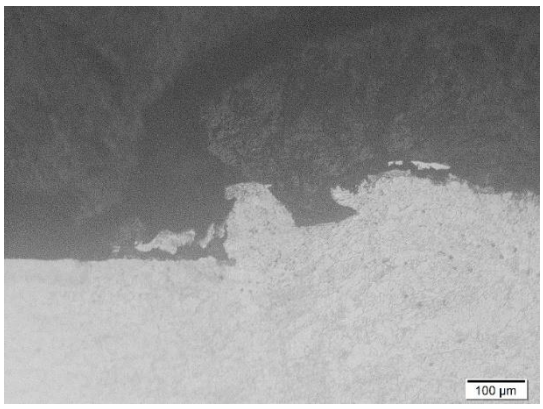

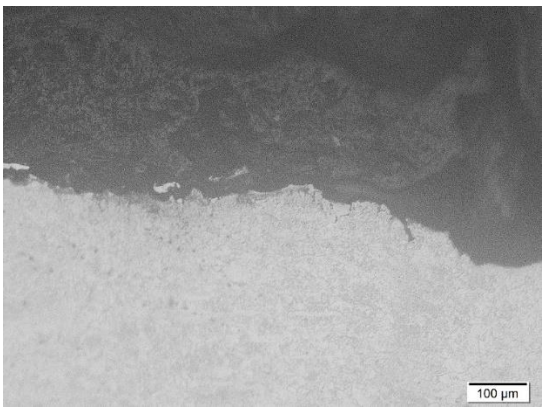

Fig. 42. *Sample 6 x10*

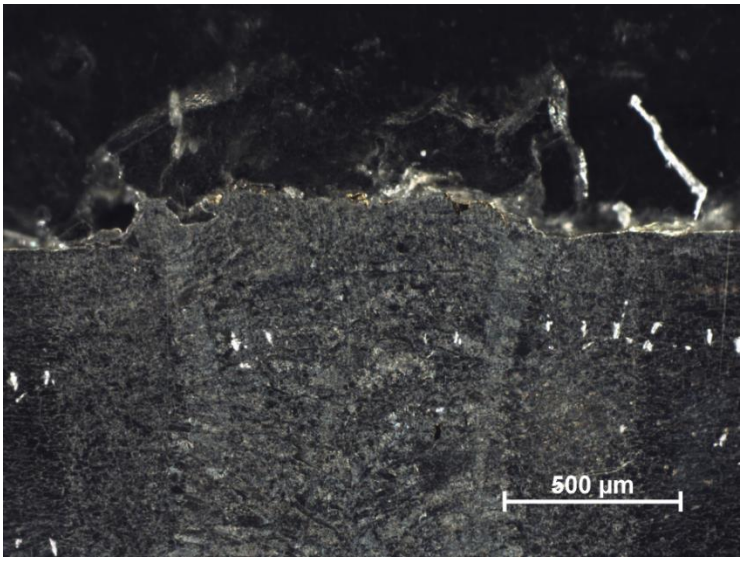

Fig. 43. *Sample 6 Cross section recorded by a stereo microscope*

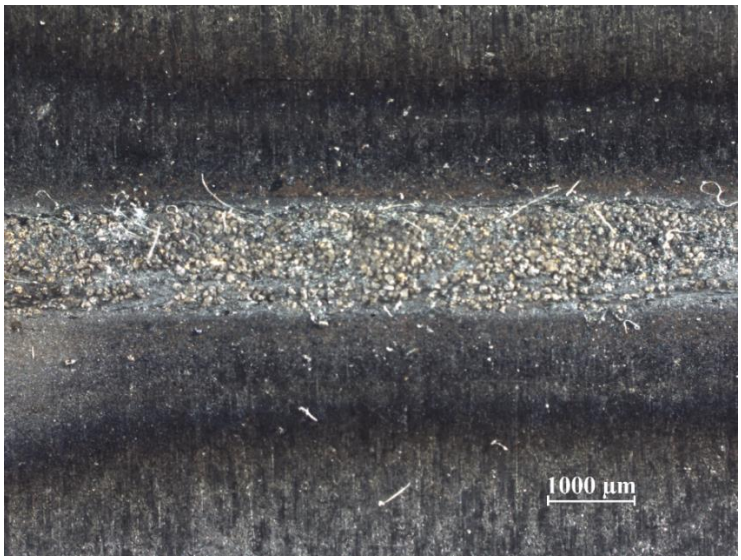

Fig. 44. *Sample 6 top surface recorded by a stereo microscope*

In this cross section there is almost no powder on top of the melt pool or inside it. Observing the image of the track taken by the Stereo Microscope, it can be seen that the powder is irregularly distributed along the track, with big areas covered by no powder. This can be due to the flow of the melt pool during the dispersing process.

Sample 7

TiN on Zinc coated steel; Front side; keyhole position; laser velocity = 3 m/min; Gas flow rate = 4 l/min

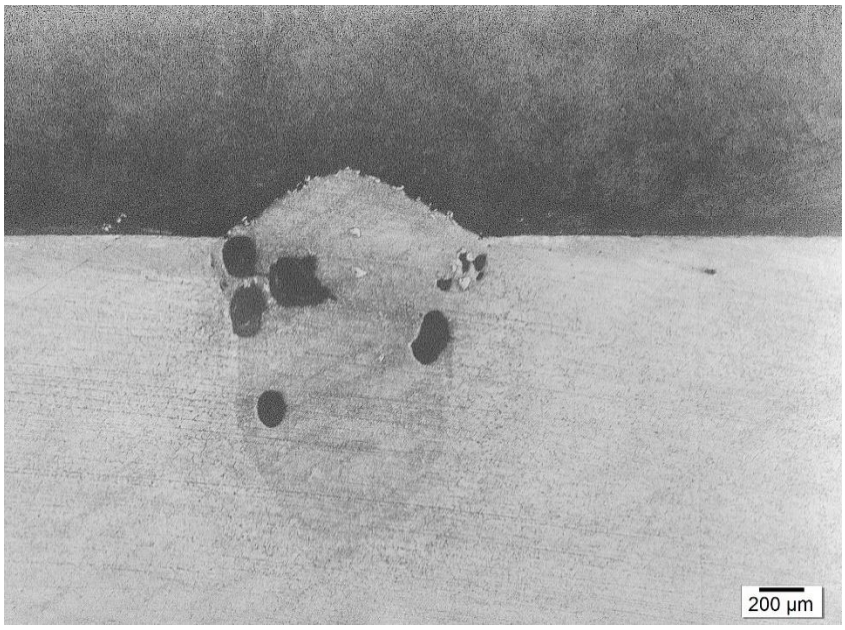

Fig. 45. *Sample 7 x2.5*

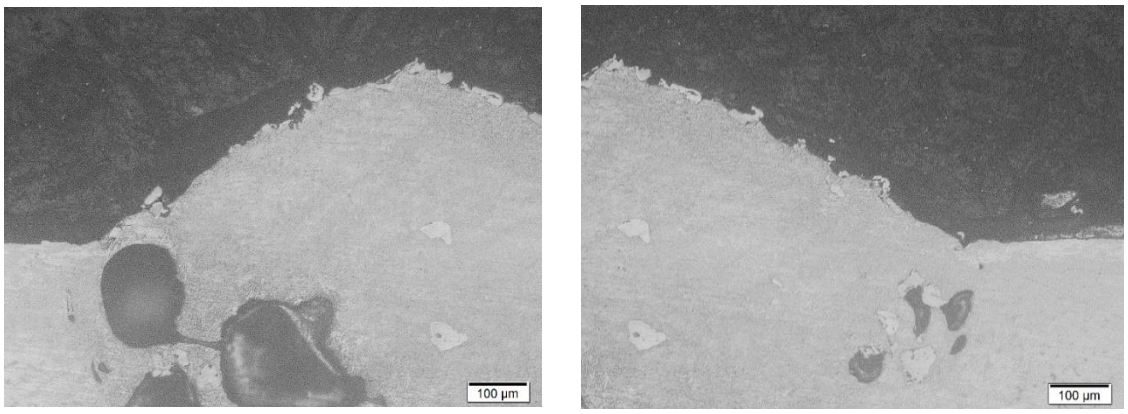

Fig. 46. *Sample 7 x10*

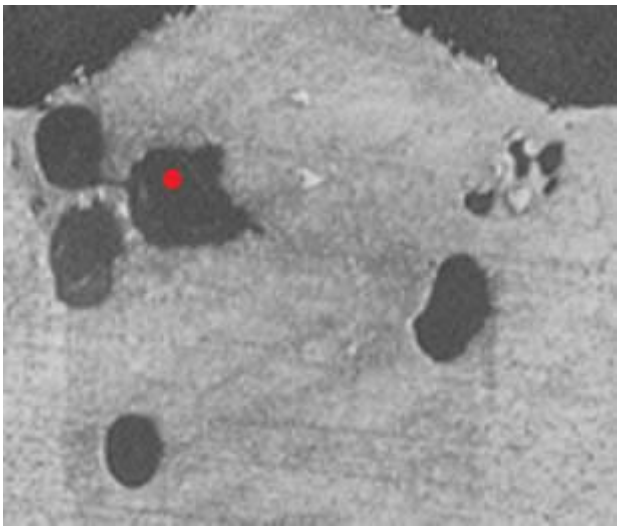

Fig. 47. *Sample 7 SEM point*

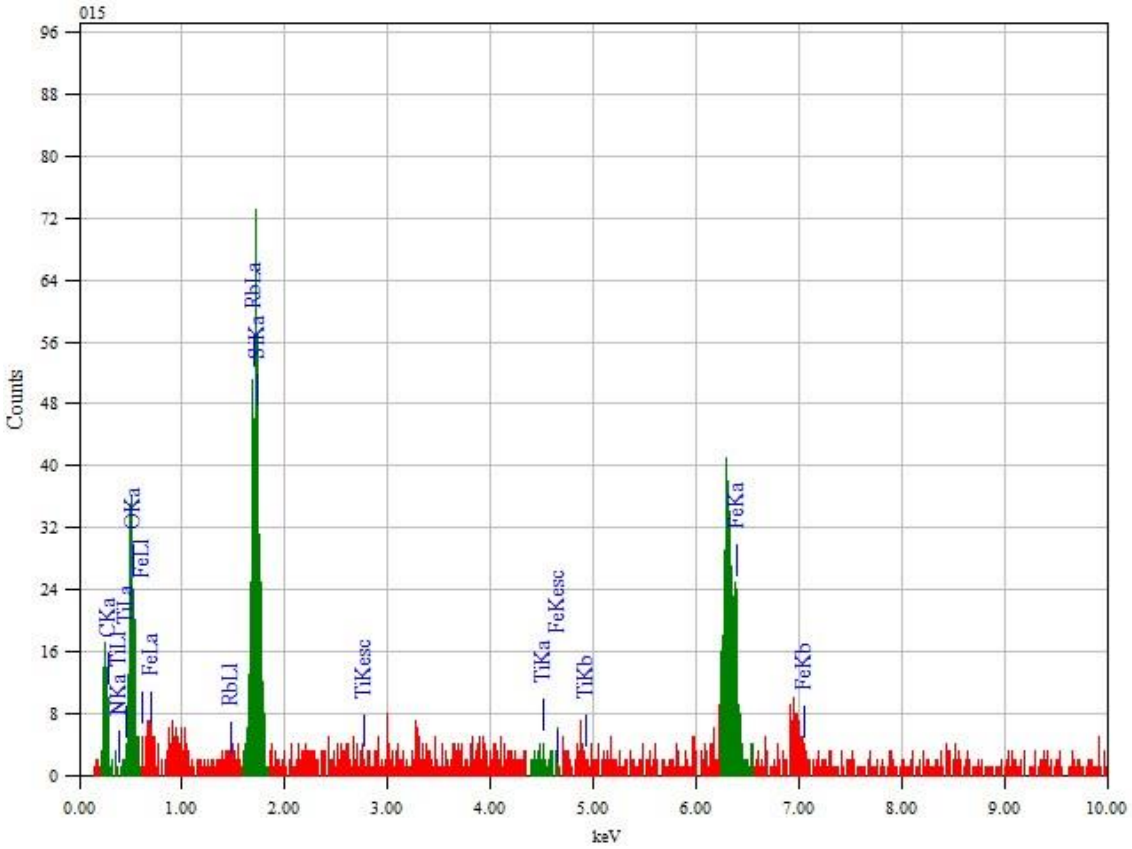

Fig. 48. *Sample 7 SEM result*

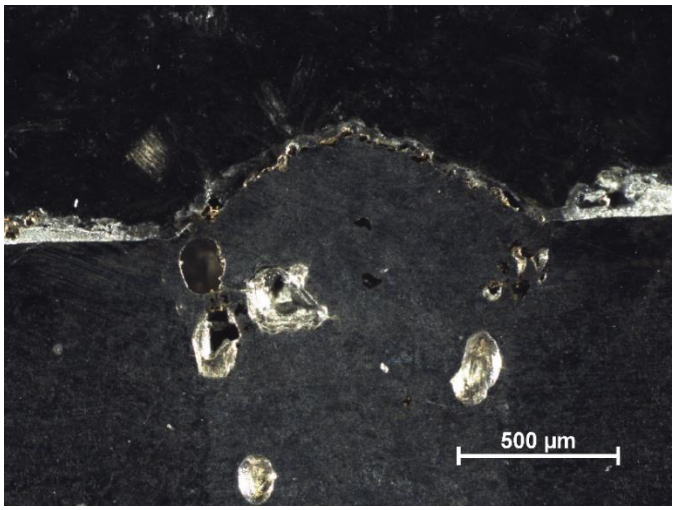

Fig. 49. *Sample 7 Cross section recorded by a stereo microscope*

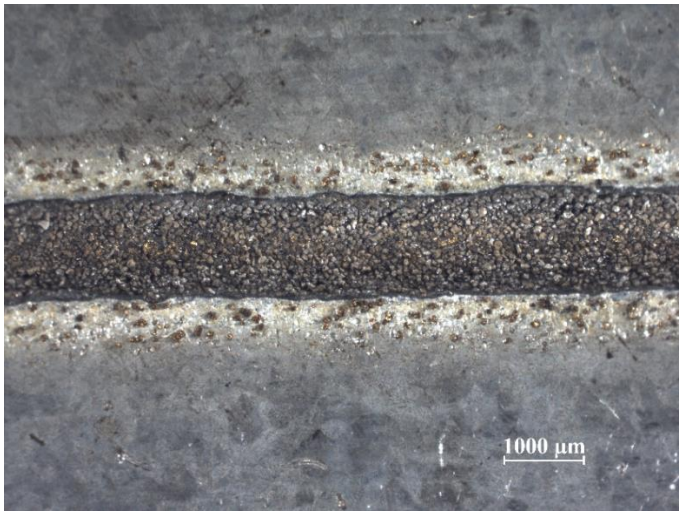

Fig. 50. *Sample 7 top surface recorded by a stereo microscope*

This sample presents what seems to be a clad layer, being especially thick in the middle, about 100 µm. Moreover, the density of powder along the track is relatively high, and the distribution is equal in all parts. However, the cross section presents big pores, similar to the ones on sample 1. The EDS results a peak of Rubidium or Silicon inside the pores. Both of these elements are not present in any of the materials used, so it might be a measurement error. In any case, the pores seem to be surrounded by a big amount of powder particles.

Sample 8

TiC on Zinc coated steel; Front side; keyhole position; laser velocity = 3 m/min; Gas flow rate = 4 l/min

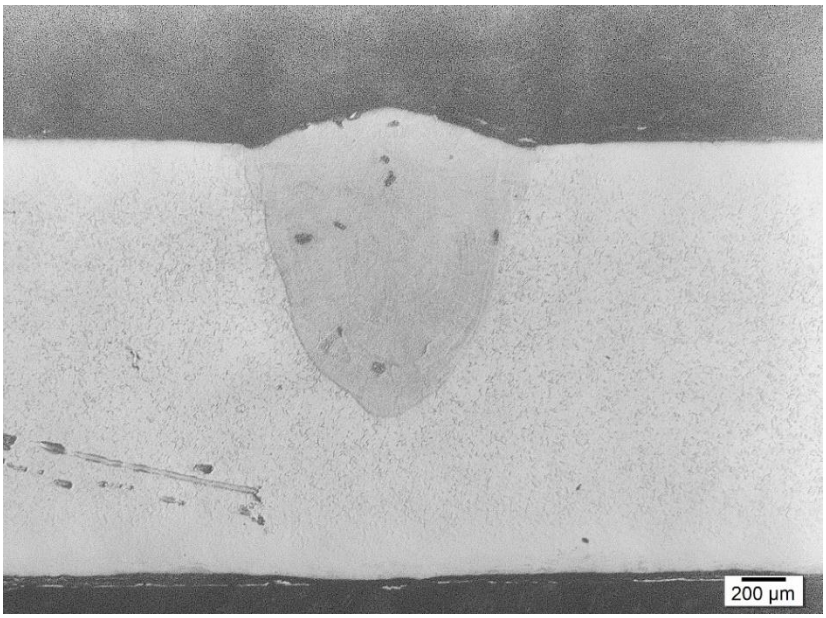

Fig. 51. *Sample 8 x2.5*

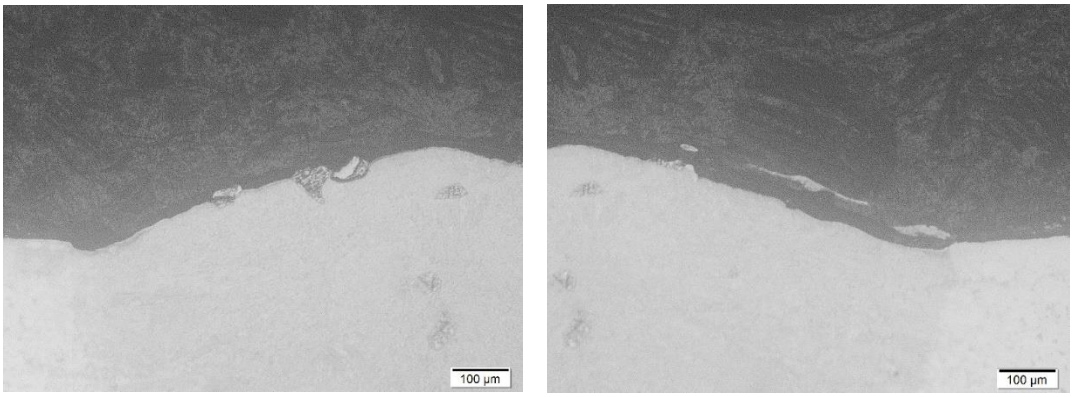

Fig. 52. *Sample 8 x10*

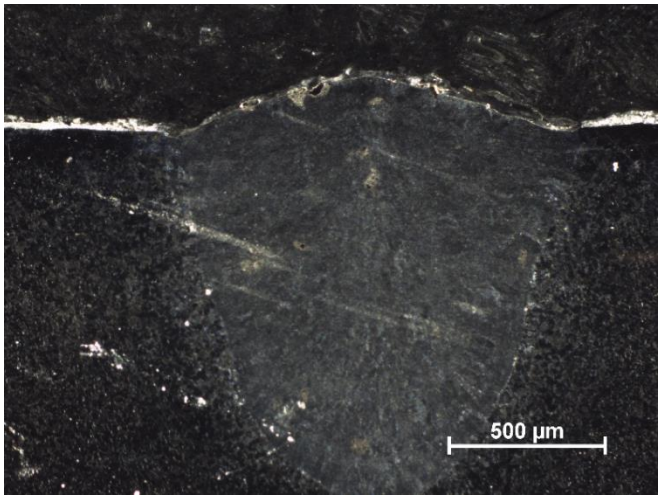

Fig. 53. *Sample 8 Cross section recorded by a stereo microscope*

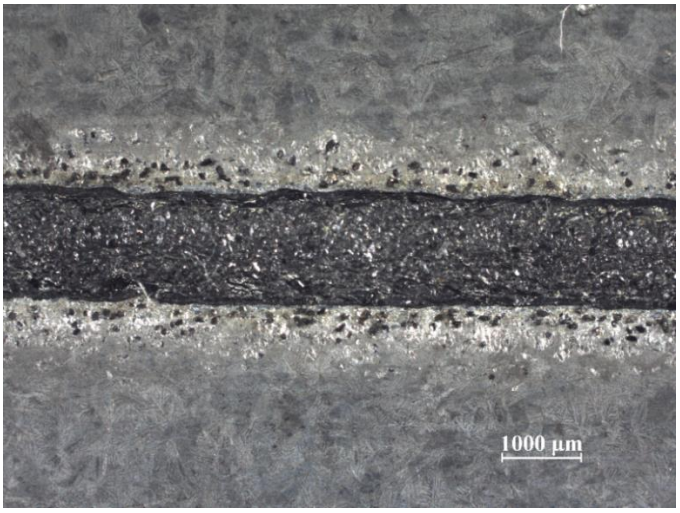

Fig. 54. *Sample 8 top surface recorded by a stereo microscope*

This track also presents an even distribution of powder along the track, as well as a 50 µm thick clad layer on top of the melt pool – which is less visible than in the previous cases due to the powder being TiC instead of TiN – and low dispersion of powder on the inside.

Sample 9

TiN on Stainless steel; Front side; keyhole position; laser velocity = 1 m/min; Gas flow rate = 4 l/min

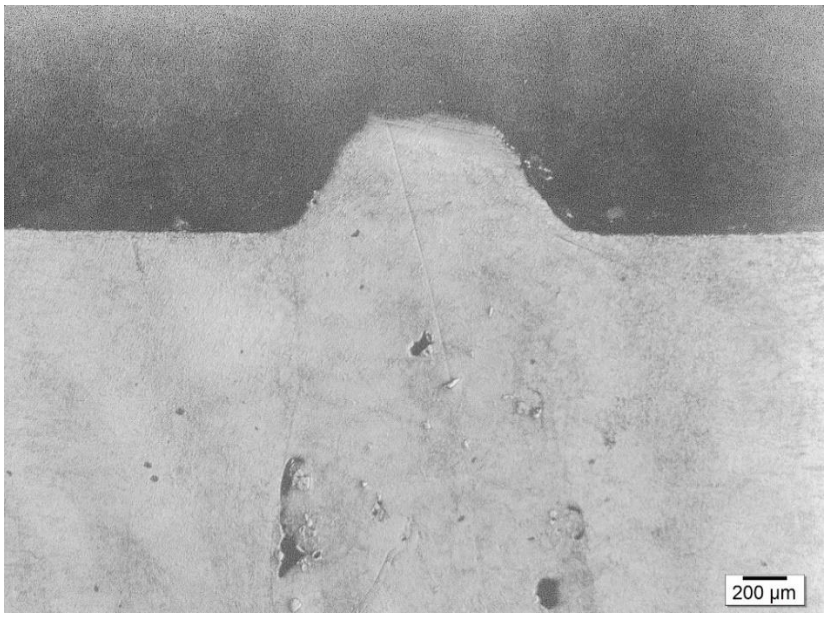

Fig. 55. *Sample 9 x2.5*

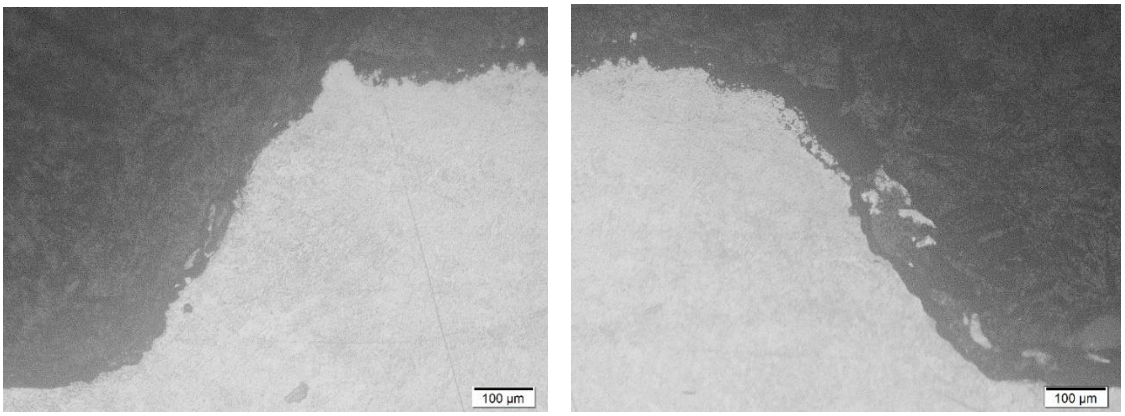

Fig. 56. *Sample 9 x10*

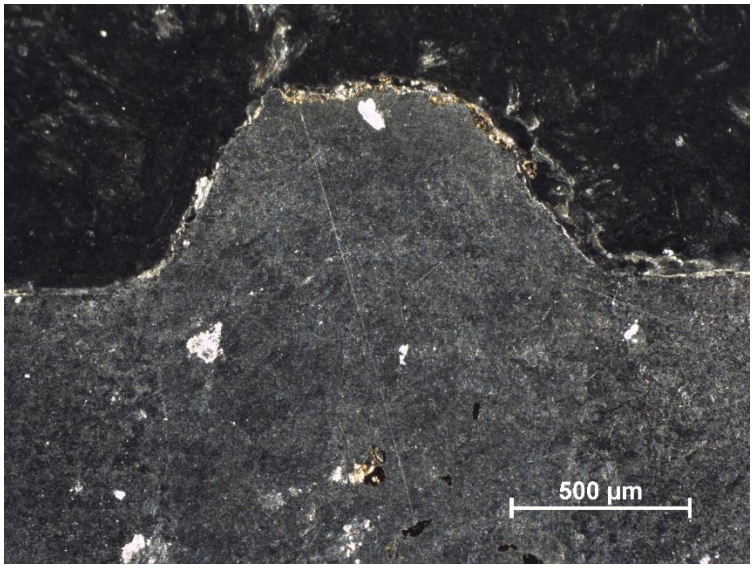

Fig. 57. *Sample 9 Cross section recorded by a stereo microscope*

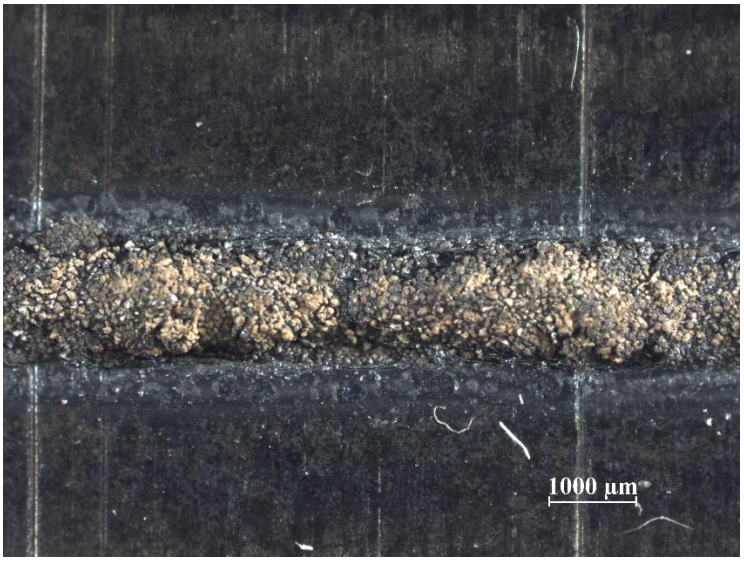

Fig. 58. *Sample 9 top surface recorded by a stereo microscope*

In this case, the melt pool presents an elevated height. The clad layer is only present in the middle part, with a thickness of 50 µm. However, the sides present no powder on them. Another noticeable aspect of this sample is that the powder seems to have melted on the top, forming a softer layer. There is also some particles of powder dispersed inside the melt pool.

Sample 10

TiC on Stainless steel; Front side; keyhole position; laser velocity = 3 m/min; Gas flow rate = 4 l/min

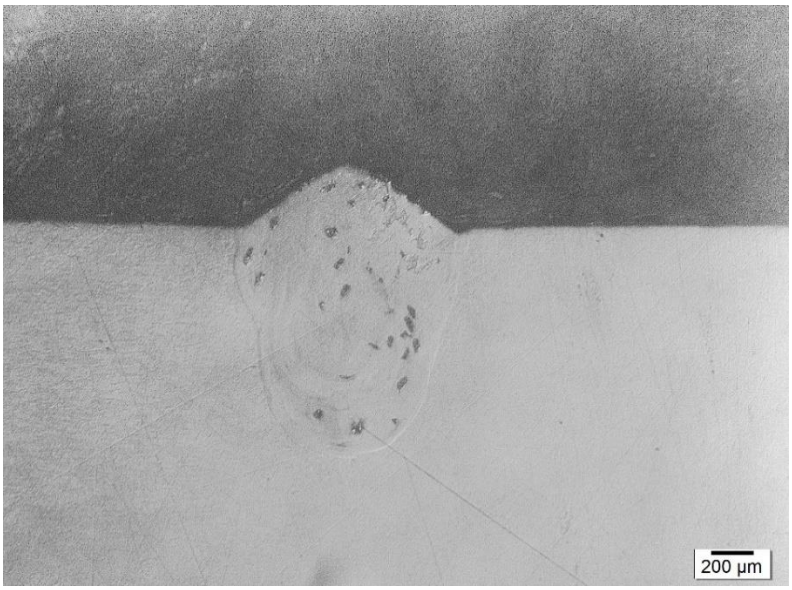

Fig. 59. *Sample 10 x2.5*

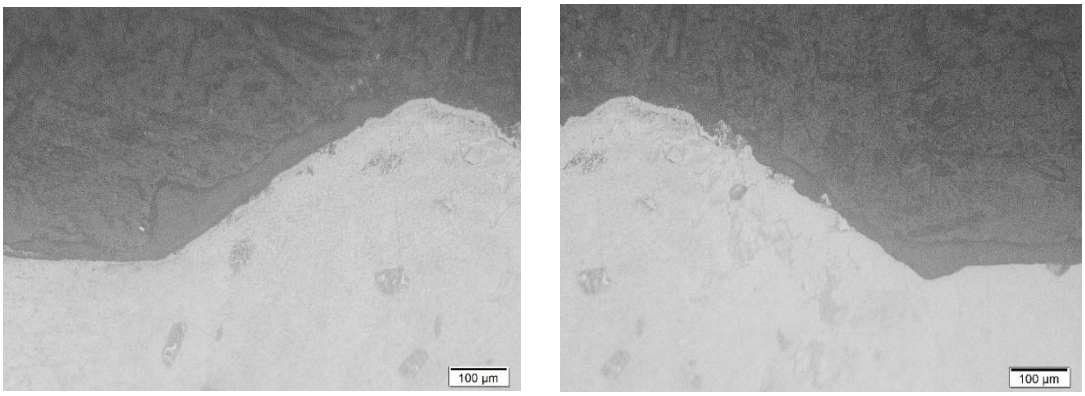

Fig. 60. *Sample 10 x10*

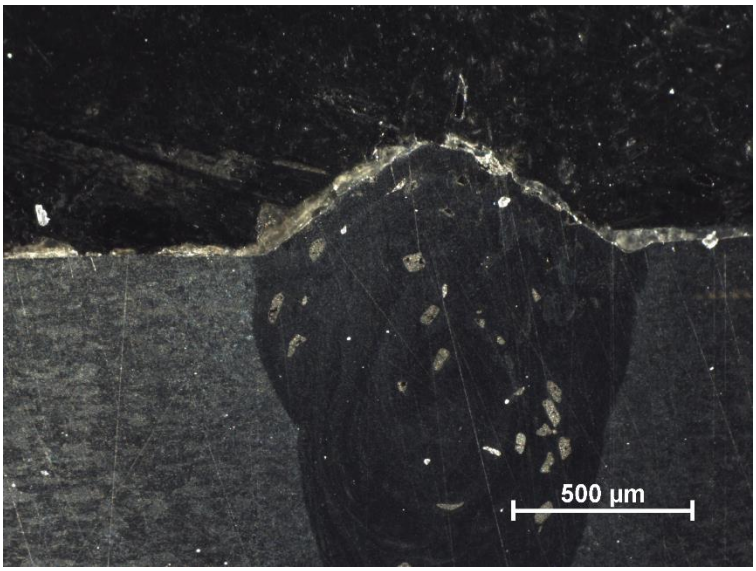

Fig. 61. *Sample 10 Cross section recorded by a stereo microscope*

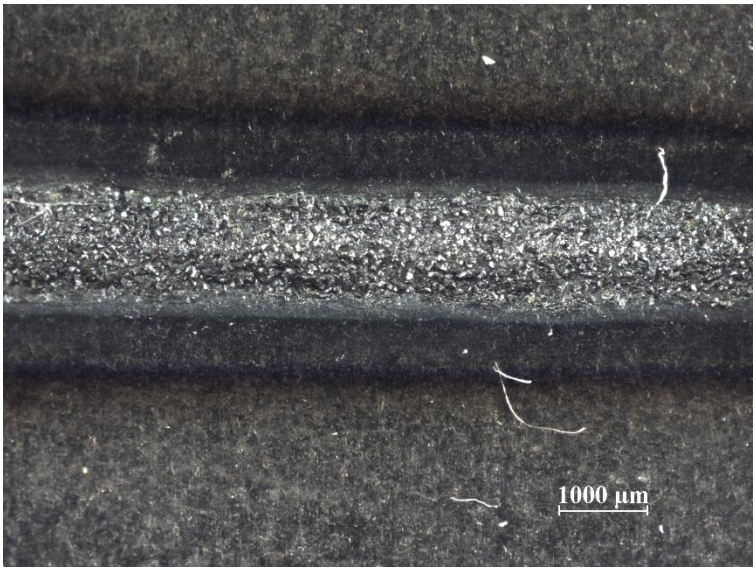

Fig. 62. *Sample 10 top surface recorded by a stereo microscope*

The cross section in this sample presents a high amount of powder dispersion inside the melt pool – the highest so far – and the clad layer is not regular across the way, as it is more present on the sides, where it presents a thickness of about 100 µm, than on the middle of the track.

Sample 11

TiN on Stainless steel; Front side; keyhole position; laser velocity = 2 m/min; Gas flow rate = 4 l/min

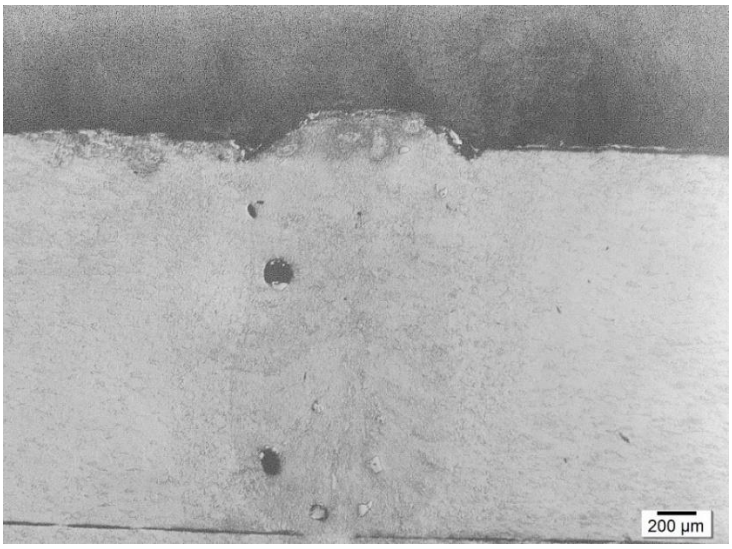

Fig. 63. *Sample 11 x2.5*

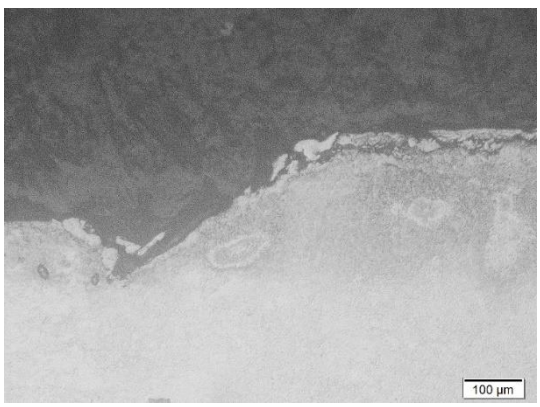

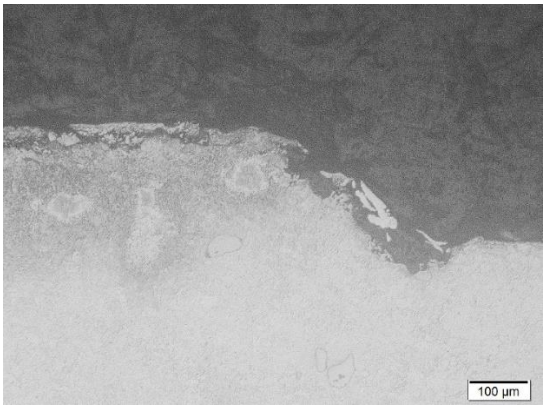

Fig. 64. *Sample 11 x10*

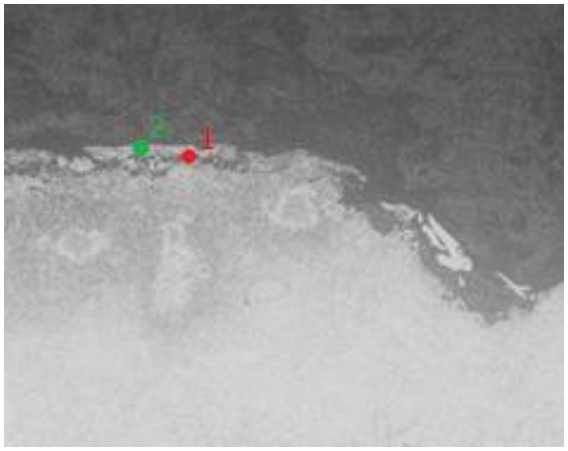

Fig. 65. *Sample 11 SEM points*

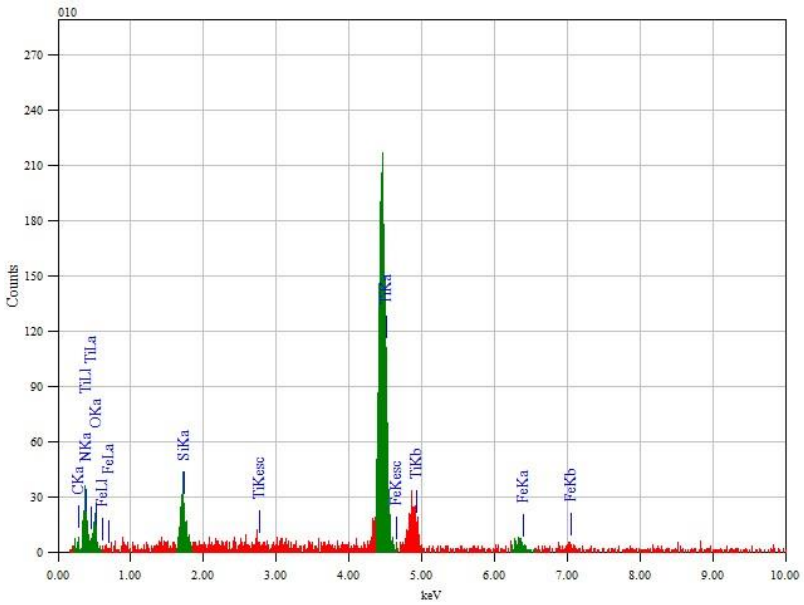

Fig. 66. *Sample 11 SEM point 1*

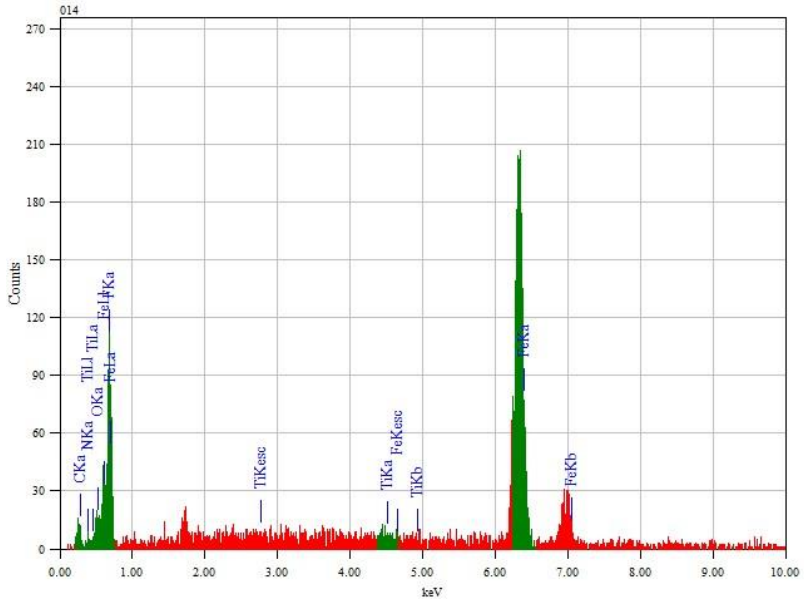

Fig. 67. *Sample 11 SEM point 2*

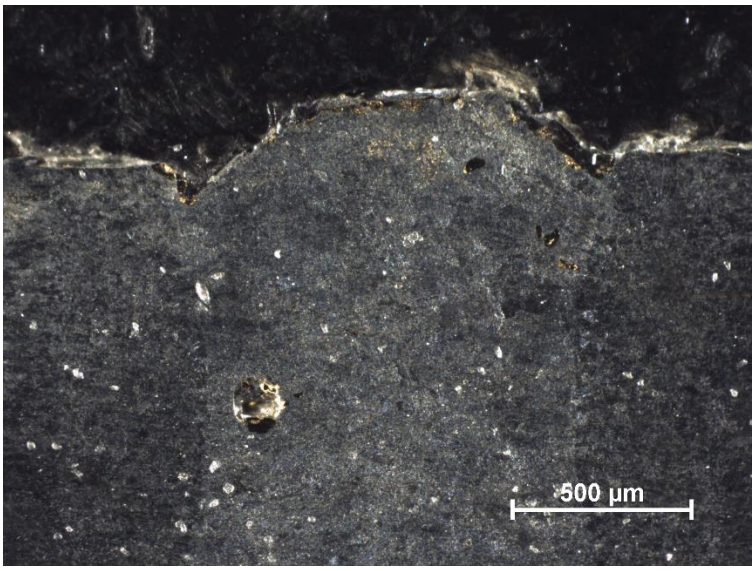

Fig. 68. *Sample 11 Cross section recorded by a stereo microscope*

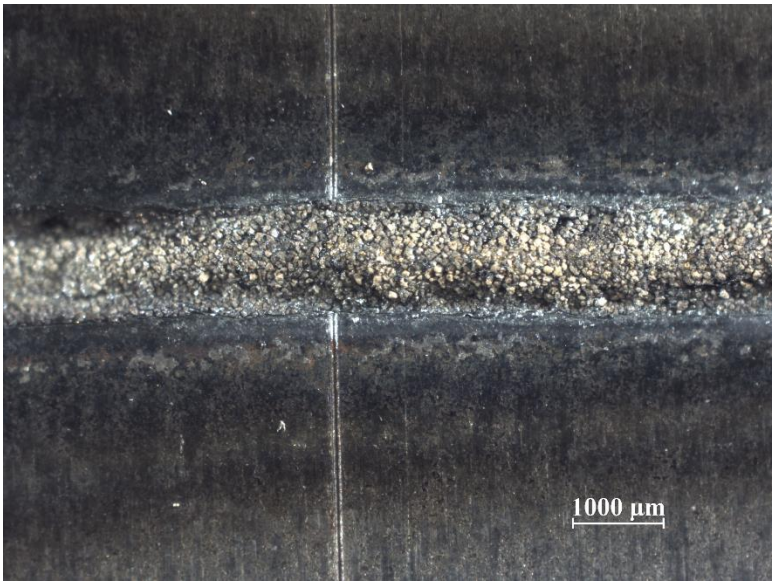

Fig. 69. *Sample 11 top surface recorded by a stereo microscope*

In this case, the powder has been melted into the surface, forming a clad layer that reaches about 100 µm of depth – as shown in the EDS results. Moreover, there are pores and powder particles in the inner parts of the melt pool.

Sample 12

TiN on Zinc coated steel; Front side; keyhole position; laser velocity = 2 m/min; Gas flow rate = 4 l/min

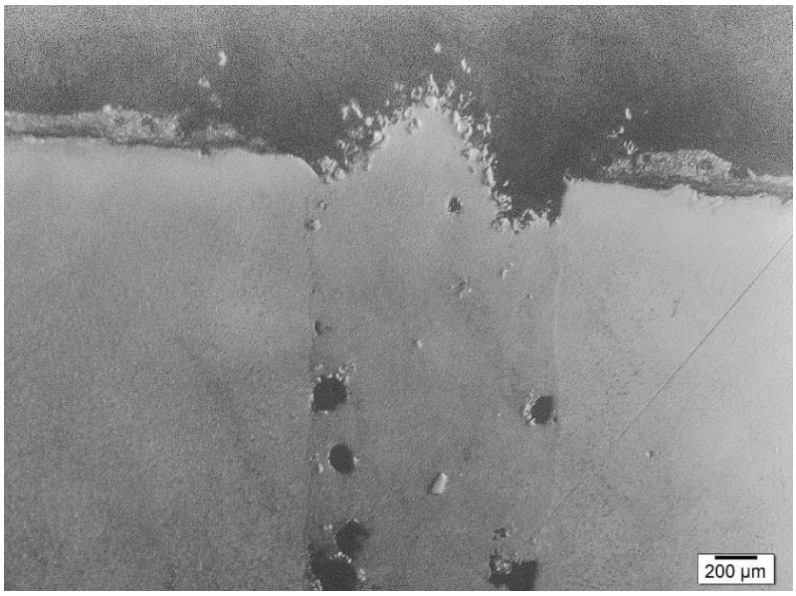

Fig. 70. *Sample 12 x2.5*

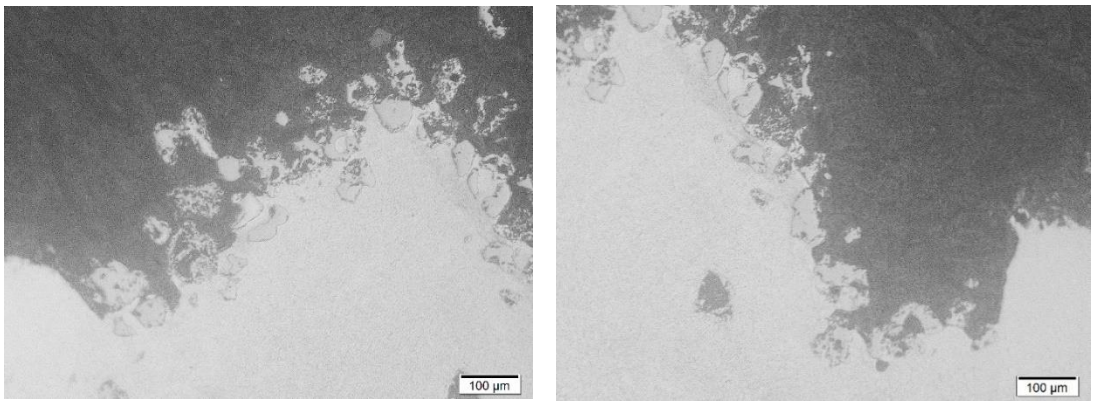

Fig. 71. *Sample 12 x10*

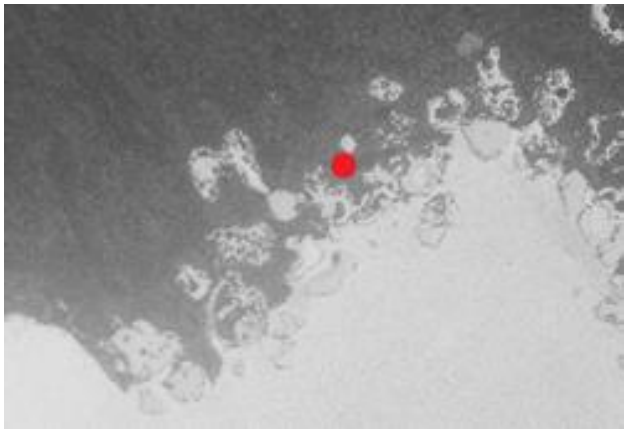

Fig. 72. *Sample 12 SEM point*

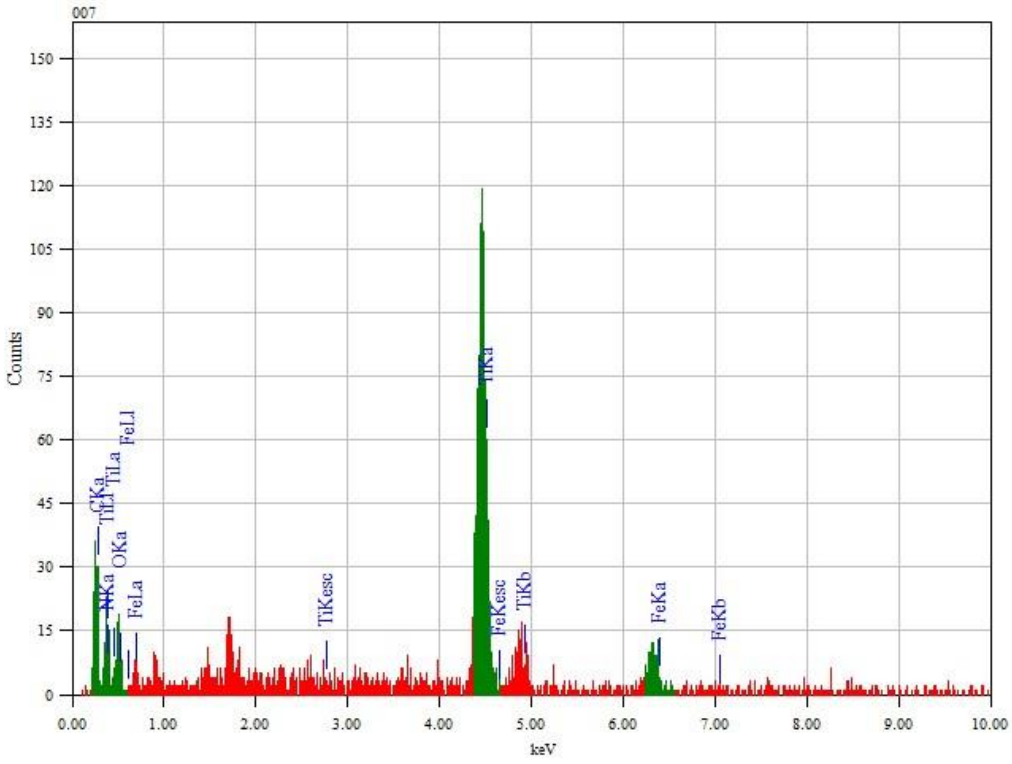

Fig. 73. *Sample 12 SEM result*

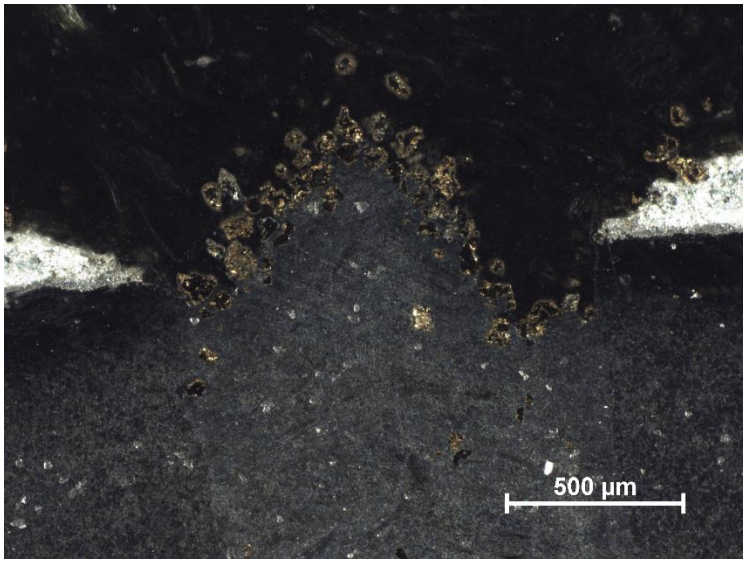

Fig. 74. *Sample 12 Cross section recorded by a stereo microscope*

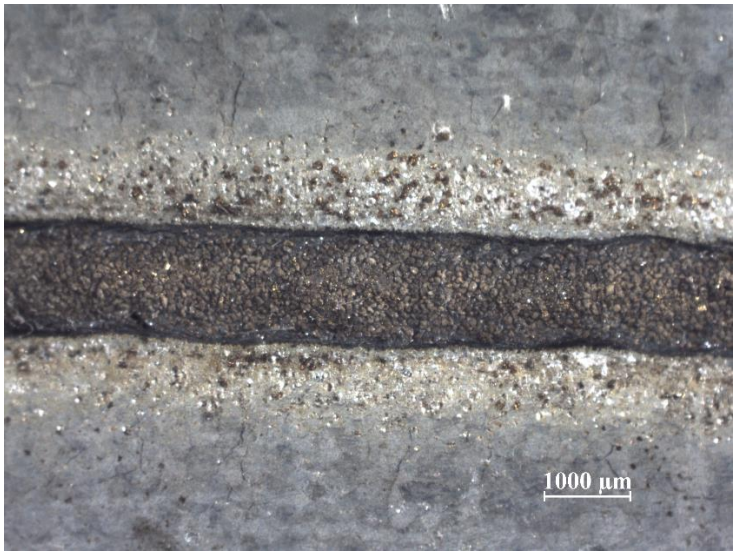

Fig. 75. *Sample 12 top surface recorded by a stereo microscope*

In this case, although there are powder particles on top of the melt pool, they have not integrated completely into it. Furthermore, the dispersion of powder outside of the melt pool has been big in this sample, as shown in the top view of the track.

Sample 13

TiC on Stainless steel; Back side; keyhole position; laser velocity = 3 m/min; Gas flow rate = 4 l/min

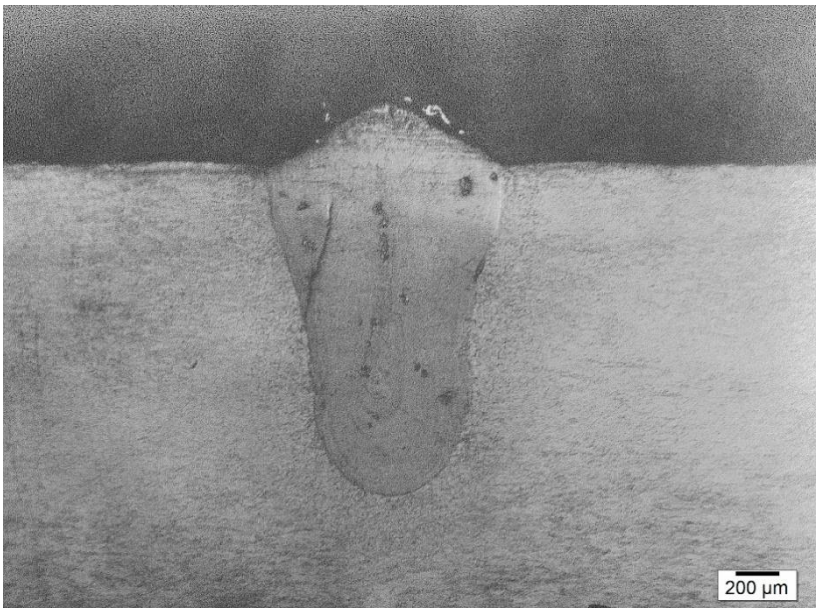

Fig. 76. *Sample 13 x2.5*

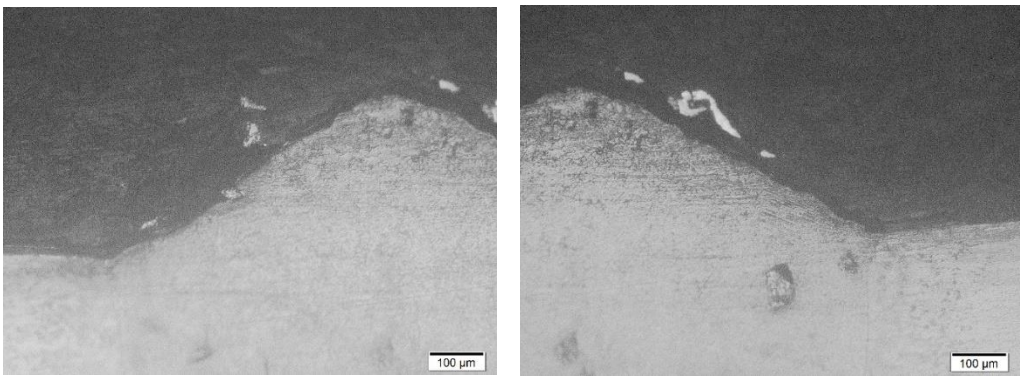

Fig. 77. *Sample 13 x10*

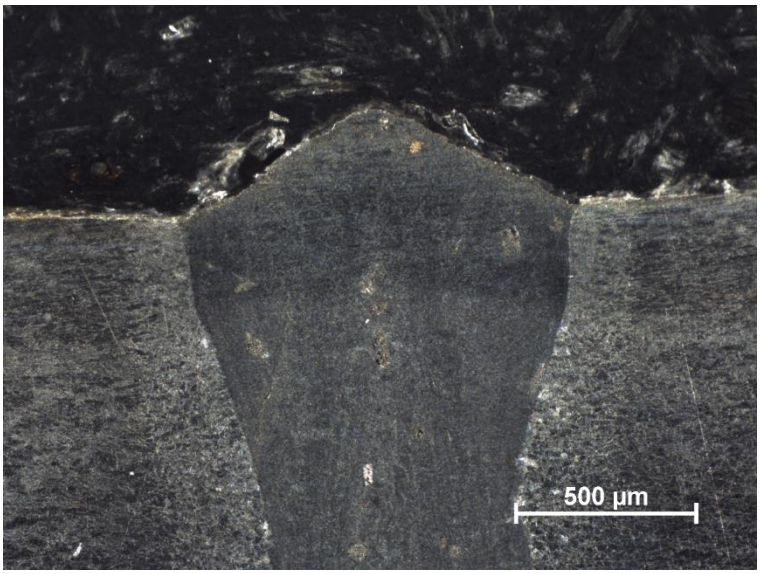

Fig. 78. *Sample 13 Cross section recorded by a stereo microscope*

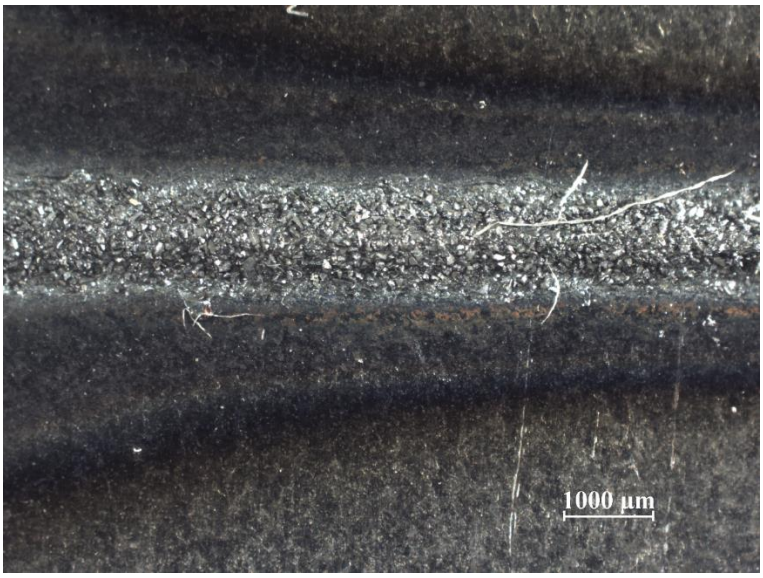

Fig. 79. *Sample 13 top surface recorded by a stereo microscope*

In this case, a clad layer seems to be present in the central and right sides of the cross section, but not in the left side. On the other hand, there is no powder dispersion inside the melt pool.

6. Discussion and conclusion

This section will include the discussion of the obtained samples, as well as the final conclusion of the project, and several suggestion for future work to research further into this topic.

6.1. Discussion

For the discussion of the different samples obtained in the process, the samples will be compared together when only one parameter changes between each other. Therefore, the influence of each parameter can be deduced.

Variation of gas flow

Sample	Gas flow (l/min)
1	17
1.2	4

Table 7. *Gas flow variation*

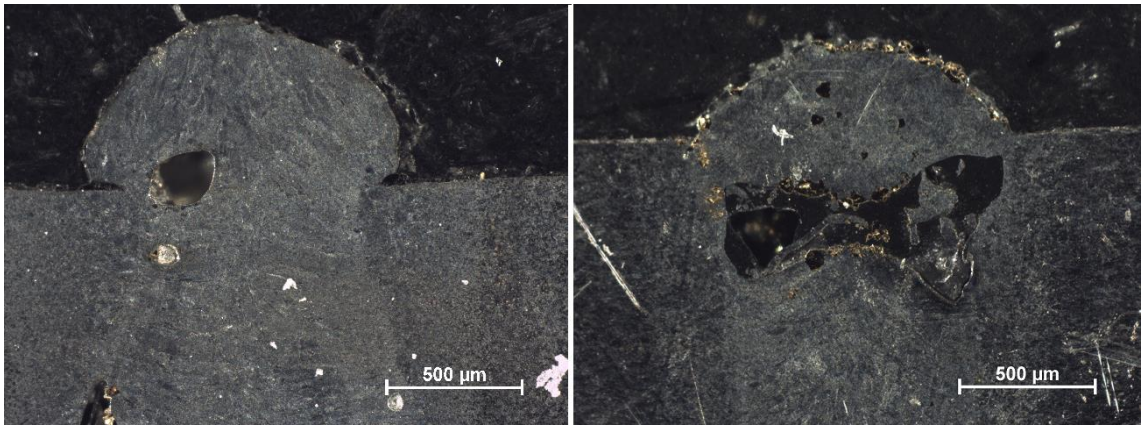

Fig. 80. *Gas flow variation – Samples 1, 1.2*

In this case, decreasing the gas flow enabled to reduce the turbulences in the melt pool, which gave the track a more regular shape,

and also contributed to agglomerate the powder particles on the surface. There is also a noticeably lower amount of powder present in sample 1 than in 1.2, although there are pores in both samples.

One possible explanation for the difference in powder quantity can be the turbulent flow in the gas nozzle. With a high gas flow, the powder that comes out of the nozzle gets spread around a larger area, instead of focusing in the keyhole, therefore resulting in a lower amount of powder present in the melt pool.

Variation of laser speed

Sample	Laser speed (m/min)
1.2	3
9	1
11	2

Table 8. *Laser speed variation*

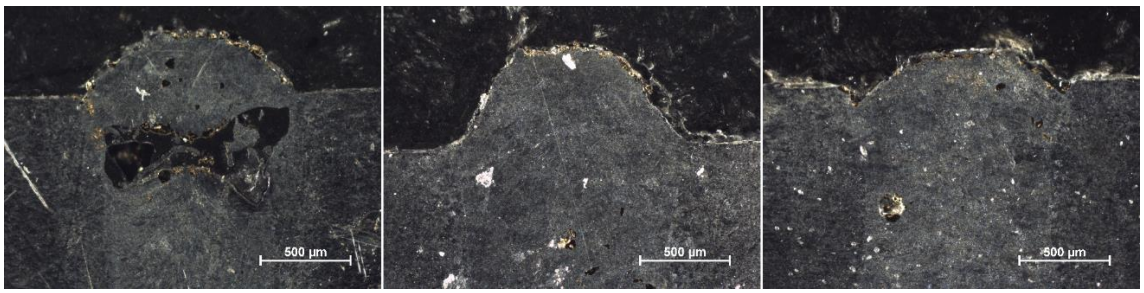

Fig. 81. *Laser speed variation – Samples 1.2, 9, 11*

In this case, the laser velocity does not seem to have caused a great impact on the powder distribution. As it can be seen here, the majority of powder particles are on the top forming a layer. However, it seems to have an effect on the state of the powder particles, as in cases 9 and 11 they seem more molten than in 1.2. This is positive, because they are less likely to come off the surface. On the other hand, there is a big porosity in sample 1.2, but it can be due to an instability of the process.

Variation of distance to keyhole

Sample	Distance to keyhole (mm)
1.2	0
2	1

Table 9. *Distance variation*

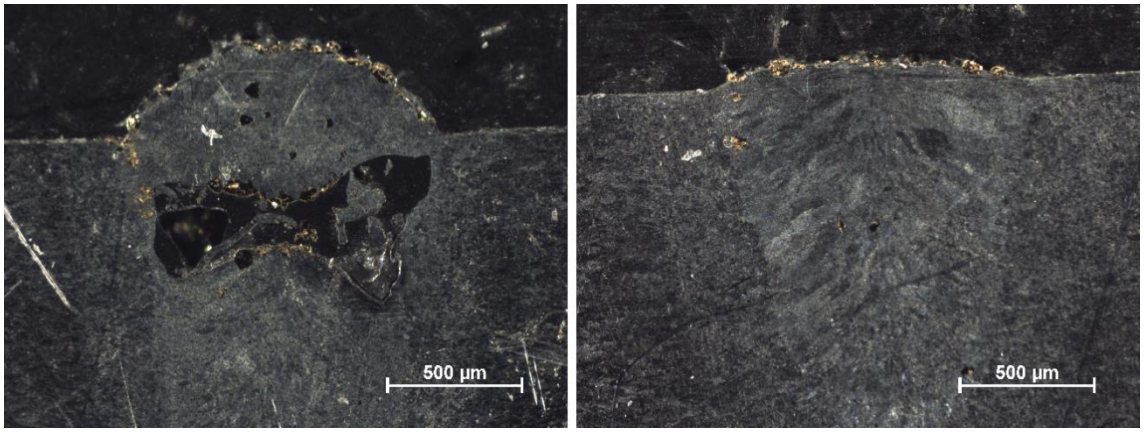

Fig. 82. *Distance variation - Samples 1.2, 2*

The distance from the nozzle to the keyhole appears to have an effect on the shape of the clad layer, being much smoother when this distance increases, as well as reducing the porosity. This is likely due to the gas pressure causing a more strong flow in the keyhole area, while if it is far, the effect will not be as powerful, therefore leading to a smoother surface. However, the amount of powder present in the melt pool decreases with the distance. This can be due to the fact that with a higher distance, the melt pool has already started to cool down then the particles hit, therefore making it difficult for the powder to remain on the surface.

Change of nozzle position

Sample	Nozzle position
10	Front
13	Back

Table 10. *Change of nozzle position*

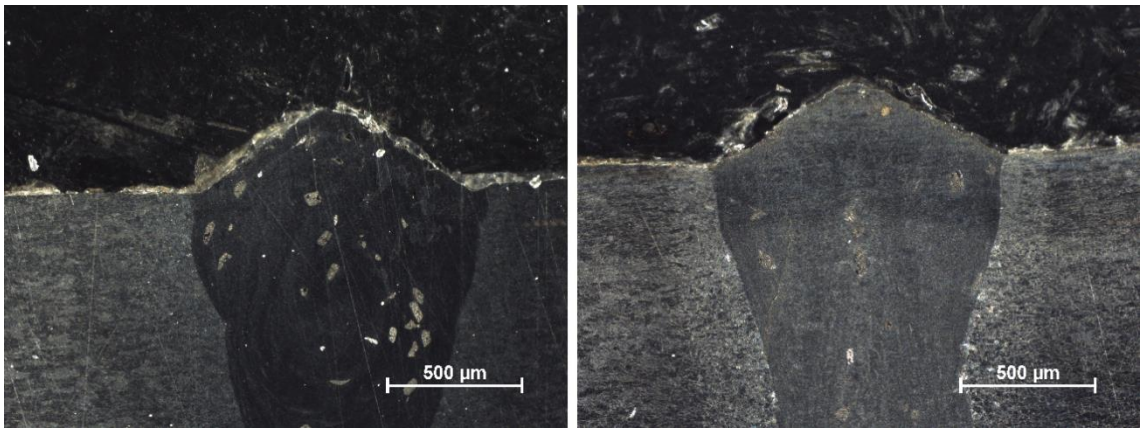

Fig. 83. *Change of nozzle position - Samples 10, 13*

The position of the nozzle does not have almost any effect on the shape of the melt pool. However, it does have an impact on the powder and its distribution. It seems that, placed on the front, the amount of powder that is deposited on the melt pool is much larger than when it is placed on the back of the laser. One possible explanation is that the powder is preheated an perhaps melted before hitting the melt pool, which improves its wetting and prevents it from rebounding This can be one of the reasons why the previous samples presented such a low amount of powder inside their melt pools.

Change of powder material

Sample	Powder material
7	TiN
8	TiC

Table 11. *Change of powder material*

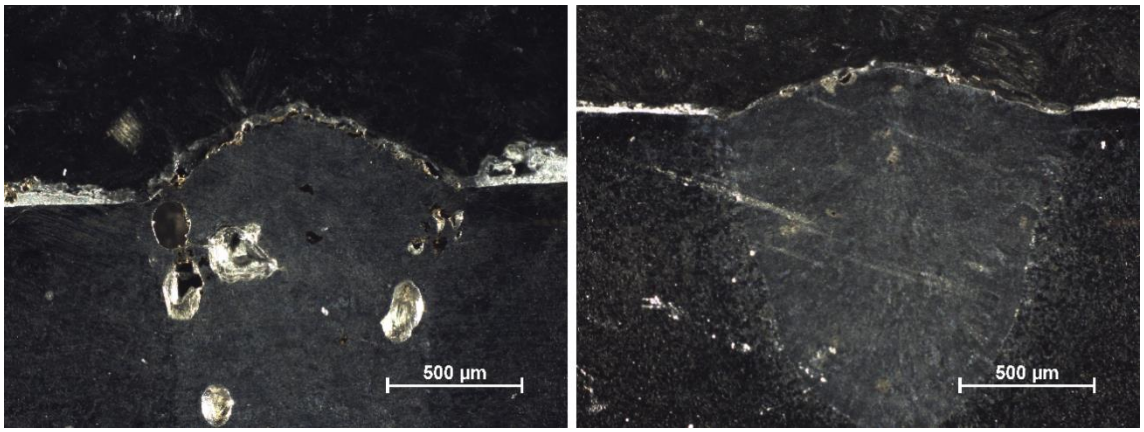

Fig. 84. Change of powder material - Samples 7, 8

The change of powder material between TiN and TiC does not have a significant impact on the result, as both powders present similar thermal properties and density. In these two images, sample 7 present big pores unlike sample 8, but that is probably a consequence of the instabilities of the process that affected the flow of the melt, rather than a consequence of the difference of powder material. Moreover, both samples show a similar clad layer on the top.

Change of base material

Sample	Base material
8	Zinc Coated Steel
10	Stainless steel

Table 12. Change of base material (1)

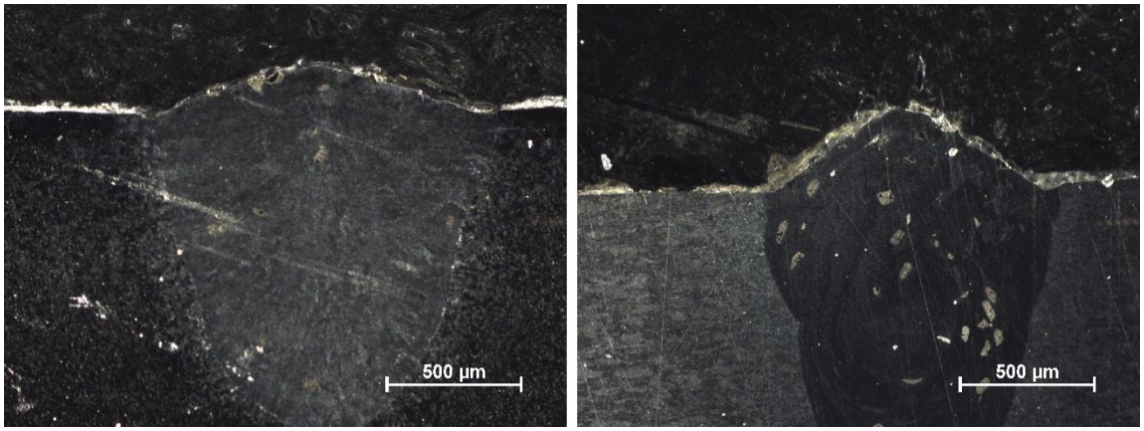

Fig. 85. Change of base material – Samples 8, 10

The stainless steel sample presents much more powder dispersed inside it than the zinc coated steel one. On the other hand, the clad layer is similar in both cases, but in the zinc coated steel case, it is more evenly distributed, while in the stainless steel there are areas where it concentrates more than others. This can be due to the thermal properties of zinc, which has a low melting point. This results in an extra liquid layer that absorbs the powder, preventing it from penetrating further inside.

Sample	Base material
11	Stainless Steel
12	Zinc coated steel

Table 13. *Change of base material (2)*

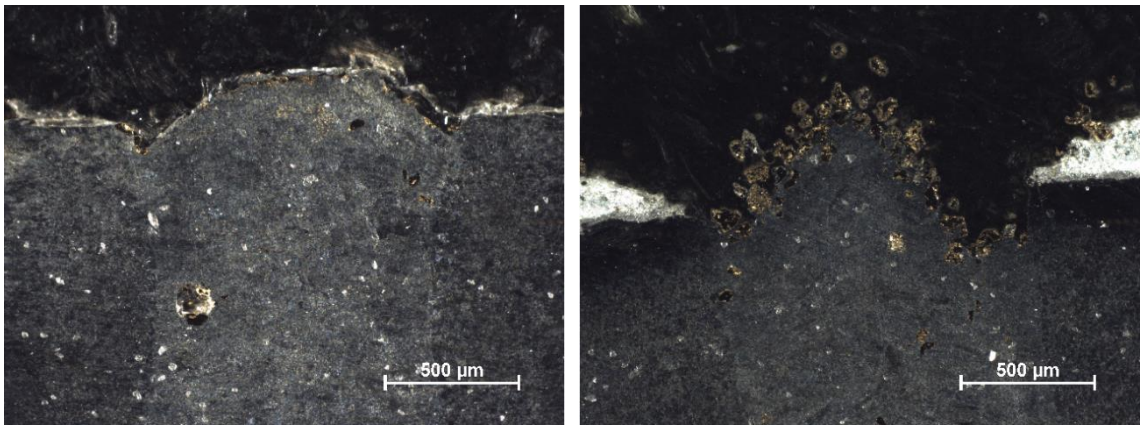

Fig. 86. *Change of base material - Samples 11, 12*

These cases present several peculiarities. Sample 11 presents a layer of base material (stainless steel) over the layer of powder, while sample 12 presents several “floating particles”. The former phenomenon can be caused by the flowing of the melt, due to the relatively low speed of the laser. On the other hand, the latter phenomenon can be due to some particles separating from the rest during the sample preparation process, as the zinc layer can also be seen slightly separated from the material. A comparison is not possible in this case due to the radically different aspect that both samples present.

6.2. Conclusion

In this project, there were several samples that presented a clad layer as desired, which a thickness that varied inside the range of the particle size (45 to 90 µm) the influence that several parameters have on the clad layer formation has been studied.

First, the increase of the gas flow seems to be negative for the formation of the layer, as well as for the deposition of powder in general. This is likely due to the instability and inaccuracy of the gas nozzle. In order to increase the amount of powder, which was the main problem in last year's samples, an increase of the rotation of the feeding table was proposed, which appears to have been positive for the goal of this experiment.

Furthermore, the influence of the base material has not proven to be a factor as significant as other ones. The Zinc coated steel seems to show a more evenly distributed clad layer, as well as less dispersion of powder into the melt pool, but the difference is not very noticeable.

As for the powder material, given the similar characteristics of the available ones (TiN and TiC), both thermal properties and density, the differences between the tests is not significant.

The laser speed does not have an impact on the powder amount, at least within this range of velocities. However, with lower speeds the powder appears to be molten, which is positive for the performance of the surface.

With larger distances to the keyhole, less powder is deposited on the surface. This is due to the quick cooling of the surface, which reduces the capacity of assimilation of the powder into the base material, and can cause some of it to bounce on top of the substrate.

However, the most significant parameter, at least in what is shown by these images, is what side of the melt pool the nozzle is placed. According to the tests, if placed on the front side, more powder is assimilated into the melt pool, which can be due to the fact that the powder arrives at the keyhole when it is still fully melted. This improves the wetting between the powder particles and the substrate. Although this can provoke more powder to disperse in the inner parts, it also helps the formation of the clad layer.

6.3. Further work

In order to gain more knowledge about the clad layer and its properties, there are some more tests that can be performed in the future, such as:

- Testing different kind of nozzles: for instance, a coaxial nozzle can experience less turbulences in the gas flow, and offer more accuracy when shooting the powder. Therefore, this way higher gas flow rates can be tested.

- More kinds of powders: Testing materials with different properties from those of TiC and TiN. WC-Co powder have shown a tendency of remaining in the upper parts of the melt pool, as well as having higher thermal conductivity and capacity. Furthermore, B_4C has a low density, which can help it to stay in the surface instead of penetrating inside.

References

1. *Impact of process parameters on particle distribution and wear resistance during laser deep alloying processes.* **Volpp, Jörg; Zingraf, Alexander; Vollertsen, Frank. 2015.**

2. *Powder particle attacthment mechanism onto liquid material.* **Volpp, J.; Prassad, H.S.; Riede, M.; Brueckner, F.; Kaplan, A.F.H. 2018.**

3. *Particle property impact on its distribution during laser deep alloying processes.* **Volpp, J.; Dietz, T.; Vollertsen, F. 2014.**

4. *Direct laser sintering of metal powders: mechanism, kinetics and microstructural features.* **Smichi, A. 2006.**

5. *Behavior of heated powder particles on solid surfaces.* **Volpp, J.; Prasad, H.S.; Kaplan, A. 2018.**

6. *https://thermtest.com/materials-database#*

7. *Binding mechanisms in selective laser sintering and selective laser melting.* **Kruth, J.P.; Mercelis, P.; Van Vaerenbergh, J. 2005.**

8. *Direct Selective Laser Sintering of Hard Metal Powders: Experimental Study and Simulation.* **Wang, X.C.; Laoui, T.; Bonse,J.; Kruth, J.P.; Lauwers, B.; Froyen, L. 2002.**

9. *Homogeneity of TiC particles distribution during laser deep dispersing (2017 project).* **Bodén, F.; Cochrane, C.; Danielsson, C., García Pérez, J.; Sarentica, A.; Torres, H. 2017.**

10. *Thin layer of particles during deep penetration laser dispersing (2018 project).* **Blanc, A.; Da Silva, A.; Förster, G.; Kelly, S.; De la Llana Pablos, J.; Pastor, A.; Tedesi, M. 2018.**

Figure sources

1. Fig.1. Dispersing regimes: https://www.mdpi.com/2075-4701/7/7/269/htm
2. Fig.2. Laser dispersing: (10)
3. Fig.3. Laser cladding: https://www.mdpi.com/2075-4701/7/7/269/htm
4. Fig.4. Difference in particle distribution: (3)
5. Fig.23. Schematic of experiment: https://en.wikipedia.org/wiki/Cladding_(metalworking)

TRABAJO FIN DE GRADO

Creación de microcapa de partículas durante dispersión profunda por láser

Resumen

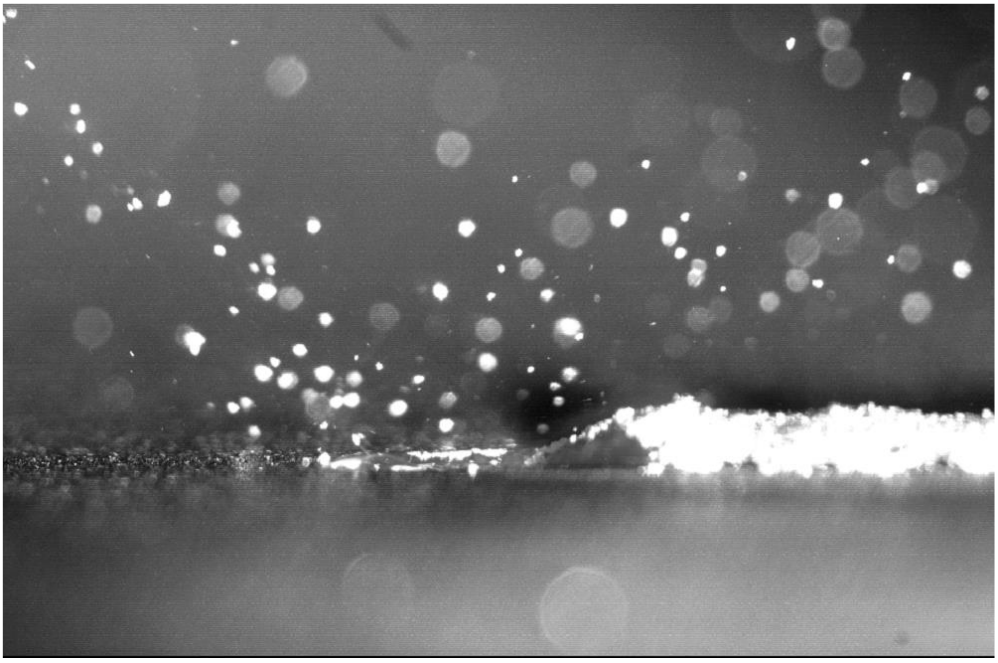

Javier De La Llana Pablos

2019

Universidad de Oviedo

Contenido

1. Introducción

1.1. Trasfondo

El revestimiento de superficies mediante láser es un proceso muy extendido, que permite la mejora de ciertas características del material tales como la resistencia al desgaste o a la corrosión, además de permitir el aumento de dureza. Esto se consigue mediante la adición de polvos de otro material con las características deseadas, tras calentar la zona con láser, creando una capa sobre el material

En experimentos anteriores se vio como es posible la formación de una microcapa de polvos del material añadido mucho más fina sobre el material base durante el proceso de dispersión profunda por láser. Esto permite la mejora de las propiedades originales, al mismo tiempo que se reduce la cantidad de material empleada para ello. Sin embargo, las condiciones que propician la formación de esta capa no son conocidas en profundidad.

1.2. Objetivo

La meta de este proyecto es alcanzar un entendimiento más profundo de las condiciones que permiten la formación de esta microcapa.

1.3. Metodología

Este proyecto consistirá en distintas partes: estudio teórico, análisis de las muestras anteriores, establecimiento de nuevos parámetros para el proceso, nuevos experimentos y el análisis de las nuevas muestras.

2. Teoría

Esta sección tratará la investigación teórica necesaria para llevar a cabo el experimento.

2.1. Dispersión por láser

En el proceso de dispersión por láser, el material en polvo es distribuido por el interior del material base fundido, para mejorar sus propiedades.

Primero, se funde el material base con el láser. Mientras el material es fundido, se añade el polvo del material a través de una boquilla, que penetra en el interior. De este modo, se consigue una distribución homogénea del polvo a lo largo de la sección transversal del recorrido del láser. Según la potencia del láser, se logrará una dispersión por conducción de calor (menos de 100 kW/cm^2) o dispersion profunda o de ojo de cerradura (más de 1 MW/cm^2).

2.2. Revestimiento por láser

Este proceso consiste en la formación de una capa del material del polvo sobre la superficie del material base. La diferencia con el proceso de dispersión es que en este caso el material base no es fundido, sino calentado. El material en polvo se añade a través de una boquilla sobre la zona afectada por el calor, y se adhieren a la superficie formando una capa superficial.

2.3. Comportamiento de las partículas en la mezcla

Ciertas propiedades del material fundido afectan a la distribución de las partículas en su interior. Por ejemplo, la tensión superficial y la viscosidad favorecen el movimiento de los polvos por su interior, mientras que perjudican la incorporación de las partículas.

Algunas condiciones para que las partículas se incorporen a la mezcla son haber absorbido la suficiente cantidad de energía del láser (ya que, si alcanza su temperatura de fusión, la interacción entre superficies líquidas es mejor que entre sólido y líquido), y alcanzar la suficiente velocidad para superar la tensión superficial del material.

2.4. Influencia de los materiales

La elección de materiales tiene gran impacto en la distribución final de las partículas a lo largo de la sección transversal.

Propiedades como una baja temperatura de fusión, alta conductividad térmica y alta absortividad de energía favorecen la incorporación de las partículas.

Las propiedades de los materiales que han sido tenidos en cuenta para este experimento, y algunos de la literatura, son:

Material	**Densidad (g/cm^3)**	**Temperatura de fusión (ºC)**	**Conductividad térmica (W/mK)**	**Capacidad calorífica (J/(mol·K))**
TiN	5.22	2930	19.2 – 56.8	37.2
TiC	4.92	3140	17.1 – 30.9	34.1
WC-Co	15.6	2850	28 – 88	54.8
TiB_2	4.52	3230	24 – 58	46.5
B_4C	2.52	2763	30 – 42	50.9
Acero (material base)	7.75 – 8.05	1300 – 1400	20 – 50	28
Zinc (recubrimiento)	7.14	420	116	25.5

Tabla 1. *Propiedades térmicas de los materiales*

En la literatura, los distintos materiales han mostrado comportamientos diferentes entre sí. Por ejemplo, las partículas de WC-Co y B_4C tienden a permanecer en las partes superiores de la sección transversal, mientras que las de TiB_2 son más propensas a una distribución homogénea.

Otras características propias de los materiales que influyen son la tensión superficial, y las distintas reacciones químicas que pueden llevar a cabo.

2.5. Influencia de los parámetros

Algunos parámetros del proceso que han sido estudiados en la bibliografía son:

- Potencia del láser: una mayor energía da lugar a la formación de un perfil de material fundido más profundo y estrecho, mientras que una menor energía provoca un perfil más ancho y superficial. Sin embargo, este parámetro no tiene un efecto significativo en la homogeneidad de la distribución de las partículas.

- Velocidad del láser: si el flujo másico del polvo es constante, una velocidad menor dará lugar a más partículas en el interior del material fundido.

- Flujo másico de polvo: depende de la velocidad de rotación del plato de alimentación, y del flujo volumétrico de gas de transporte. Un mayor flujo de gas produce una distribución más profunda de las partículas. Por el otro lado, un aumento de la velocidad del plato provoca un crecimiento en el número de partículas presentes dentro del material fundido.

2.6. Resultados de experimentos anteriores

En los experimentos llevados a cabo en la Universidad Tecnológica de Luleå en los dos años anteriores, los resultados fueron:

- En el proyecto de 2017 (*Homogeneity of TiC particles distribution during laser Deep dispersing*) en el que se usaron partículas de TiC sobre acero Hardox 450 variando la velocidad del láser y el flujo de gas. Algunas muestras de este experimento revelaron la microcapa de polvo sobre el material base.

- En el proyecto de 2018 (*Thin layer of particles during deep penetration laser dispersing*) se usaron dos tipos de partículas: TiN y TiC, sobre dos materiales base: acero inoxidable y acero recubierto de zinc, variando parámetros como la velocidad del proceso y el flujo del gas. Se concluyó que la capa formada sobre el acero recubierto de zinc era más consistente pese a presentar mayor porosidad en el interior. Además, una baja velocidad y un bajo flujo de gas parecían favorecer la formación de la capa de revestimiento.

3. Análisis de muestras anteriores

En esta sección se estudiarán las muestras que no fueron analizadas durante el proyecto de 2018, puesto que podrían dar información útil de cara a los nuevos experimentos.

3.1. Parámetros del proceso

6 muestras del anterior experimento (correspondientes a las numeradas como 6, 7, 8, 9, 10 y 12) han sido analizadas en este proyecto.

Los parámetros del proceso fueron:

Diámetro de la fibra	0.4 mm
Lente convergente	250 mm
Lente colimadora	150 mm
Diámetro del rayo	0.67 mm
Ángulo de la boquilla	40-45º
Velocidad del plato	2 rpm
Potencia del láser	3 kW
Flujo másico (TiN)	6.8 g/min
Tamaño de partícula (TiN)	-90+45 µm

Tabla 2. *Parámetros del proceso constantes*

Muestra	Polvo	Velocidad del láser (m/min)	Flujo de gas (l/min)	Material base
6	TiN	3	6	Acero inoxidable
7	TiN	3	8	Acero inoxidable
8	TiN	3	4	Acero inoxidable
9	TiN	2	4	Acero inoxidable
10	TiN	4	4	Acero inoxidable
12	TiN	3	4	Acero recubierto de zinc

Tabla 3. *Parámetros del proceso variables*

3.2. Preparación de la muestra

Para su observación, las muestras fueron cortadas, montadas, limadas y tratadas con ácido 3% Nital, con el objetivo de mejorar la distinción entre los distintos componentes de la microestructura.

3.3. Observación de la muestra

Para su estudio, la sección transversal de las muestras fue observada a través de un microscopio óptico. También se estudiaron diversos puntos de la muestra 6 mediante un microscopio electrónico de barrido.

Las imágenes obtenidas son las siguientes:

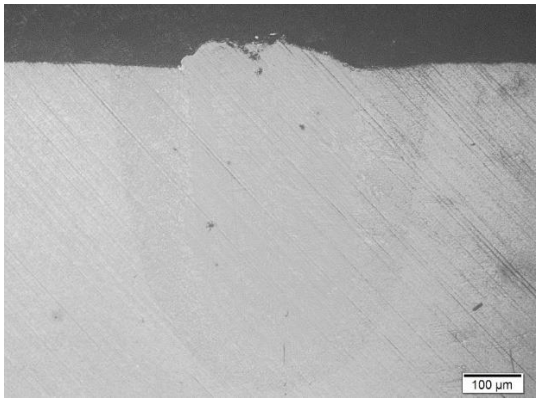

Fig. 1. *Muestra 6*

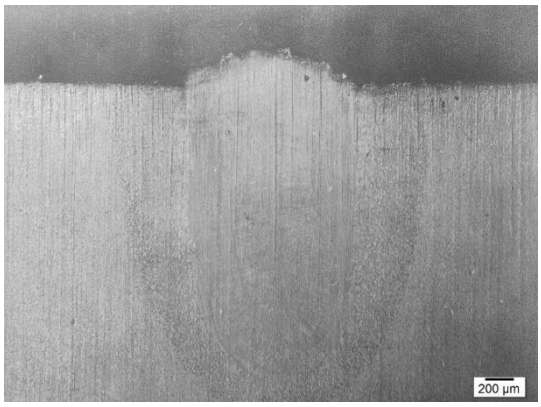

Fig. 2. *Muestra 7*

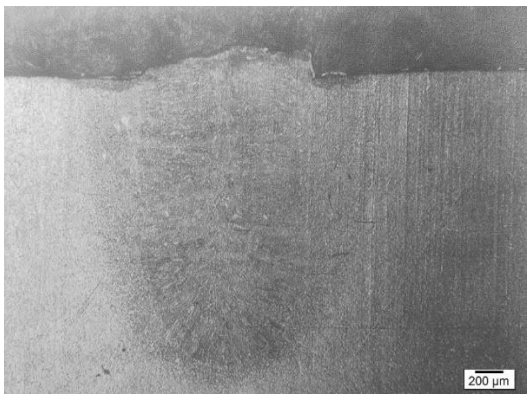

Fig. 3. *Muestra 8*

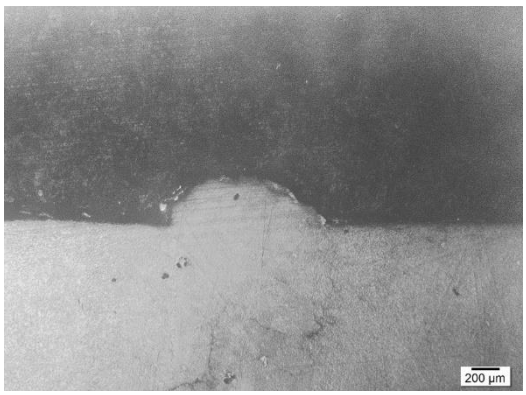

Fig. 4. *Muestra 9*

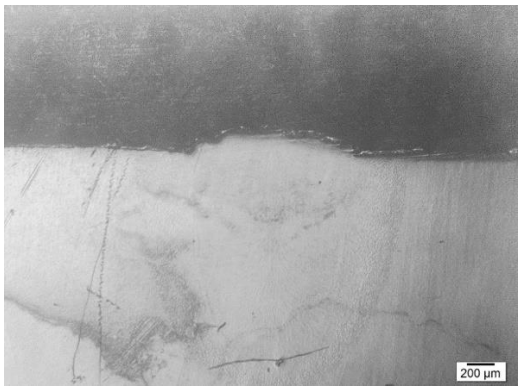

Fig. 5. *Muestra 10*

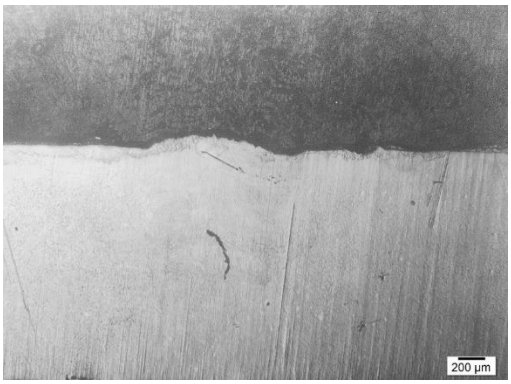

Fig. 6. *Muestra 12*

3.4. Discusión

Comparando entre sí las muestras, se puede concluir lo siguiente:

- El flujo de gas no afecta la cantidad de polvo presente en la sección, pero sí la distribución, ya que el polvo penetra más con un flujo de gas mayor.

- La velocidad del láser no muestra un gran impacto, pues todas las muestras presentan muy poca cantidad de polvo en ellas.

- No hay diferencias importantes entre la distribución de TiN y la de TiC, ya que sus características son similares.

- El acero recubierto de zinc no presenta grandes diferencias respecto al inoxidable.

- La conclusión principal es que el mayor problema es la poca cantidad de polvo presente en las muestras, por lo que los futuros experimentos deben centrarse en aumentarla.

4. Nuevos experimentos

En esta sección se tratará la metodología empleada para obtener las nuevas muestras.

4.1. Variación de parámetros

Como se ha visto en los análisis anteriores, el mayor problema es la escasez de partículas de polvo presente en las muestras. Por ello, algunas medidas que se adoptarán son:

- Se incrementará el ángulo de la boquilla para reducir la influencia de la tensión superficial. También se probará a colocar la boquilla a diferentes distancias del ojo de cerradura en el material base, y a colocarlo en varias posiciones (delante y detrás del mismo).

- Se mantendrán los materiales del experimento anterior (TiN y TiC para polvo, acero inoxidable y acero recubierto de zinc para el material base).

- La velocidad del láser será variada en un rango bajo (2 – 3 m/min)

- Para aumentar el flujo másico de partículas, en lugar de aumentar el flujo de gas (que se mantendrá a un nivel bajo de 4 l/min) se incrementará la velocidad rotacional del plato de alimentación, con el objetivo de alcanzar un flujo másico de 10 g/min.

4.2. Plan experimental

Los parámetros utilizados fueron:

Diámetro de la fibra	0.4 mm
Lente de convergencia	250 mm
Lente colimadora	150 mm
Diámetro del rayo	0.67 mm
Ángulo de la boquilla	52º
Distancia de la boquilla al láser	X: 6 mm (+ posición); Y: 6 mm
Velocidad rotacional del plato	2.75 rpm
Flujo másico	10 g/min
Tamaño de partícula (TiN)	-90+45 µm
Tamaño de partícula (TiC)	-90+45 µm

Tabla 4. *Parámetros constantes*

Muestra	Lado de la boquilla	Posición de la boquilla	Material de polvo	Material base	Velocidad del laser (m/min)	Flujo del gas (l/min)
1*	Delante	cerradura	TiN	Acero inoxidable	3	17
1.2	Delante	cerradura	TiN	Acero inoxidable	3	4
2	Delante	1 mm	TiN	Acero inoxidable	3	4
3	Delante	2 mm	TiN	Acero inoxidable	3	4
4*	Detrás	cerradura	TiN	Acero inoxidable	3	17
5*	Detrás	1 mm	TiN	Acero inoxidable	3	17
5.2	Detrás	1 mm	TiN	Acero inoxidable	3	4
6	Detrás	2 mm	TiN	Acero inoxidable	3	4
7	Delante	cerradura	TiN	Acero cub. de zinc	3	4
8	Delante	cerradura	TiC	Acero cub. de zinc	3	4
9	Delante	cerradura	TiN	Acero inoxidable	1	4
10	Delante	cerradura	TiC	Acero inoxidable	3	4
11	Delante	cerradura	TiN	Acero inoxidable	2	4
12	Delante	cerradura	TiN	Acero cub. de zinc	2	4
13	Detrás	cerradura	TiC	Acero inoxidable	3	4

Tabla 5. *Parámetros variables*

***Nota:** las muestras 1, 4 y 5 se realizaron accidentalmente con un flujo de gas de 17 l/min debido a errores durante la calibración.

4.3. Metodología experimental

El experimento fue llevado a cabo con un láser Yb:YAG, que contaba con una mesa de movimiento 3d para colocar las muestras. Junto al láser se colocó la boquilla del polvo, conectada a la mesa de alimentación y al gas de transporte.

También se instaló una cámara HSI (High Speed Imaging) para grabar el proceso.

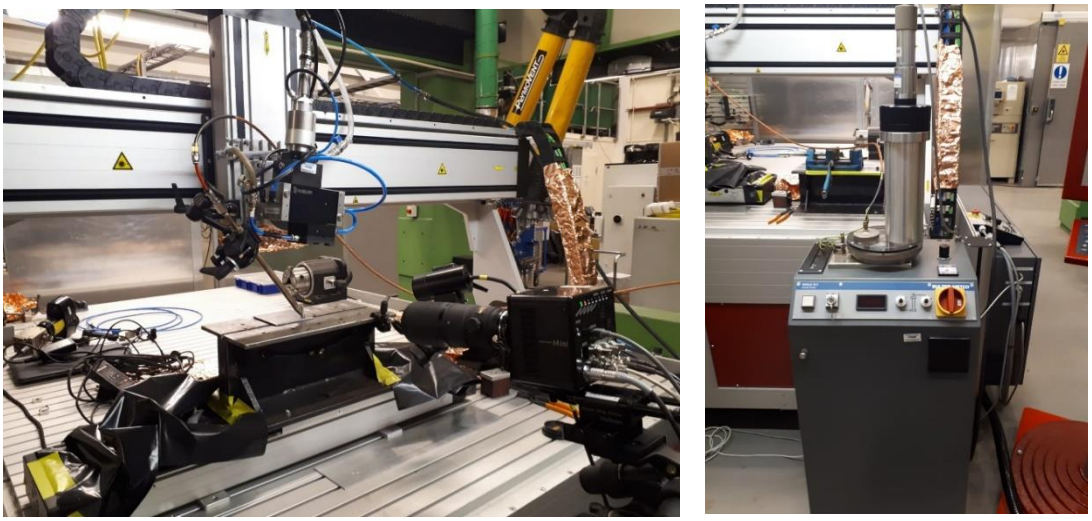

Fig. 7. *Fotografías del experimento*

5. Análisis de las nuevas muestras

En esta sección se tratará el estudio de las nuevas muestras obtenidas.

5.1. Preparación de muestras

Las muestras fueron preparadas de manera similar a como lo fueron las anteriores: fueron cortadas por la sección transversal central, montadas, limadas, y tratadas con ácido 3% Nital.

Fig. 8. *Muestras*

En esta ocasión, las muestras 3, 4, 5 y 5.2 presentaban una distribución de polvo irregular a lo largo del recorrido, y ausencia de material fundido en algunas zonas, por lo que no fueron estudiadas en este proyecto.

5.2. Observación de muestras

Al igual que en las muestras anteriores, en esta ocasión la sección transversal central fue observada. Para ello se empleó un microscopio óptico.

A continuación, se observaron tres de las muestras (7, 11 y 12) a través de un SEM para estudiar ciertas zonas del material.

Finalmente, las muestras fueron observadas por un estereomicroscopio con cámara incorporada, el cual permite tomar fotografías a color. Estas imágenes son las que se encuentran a continuación.

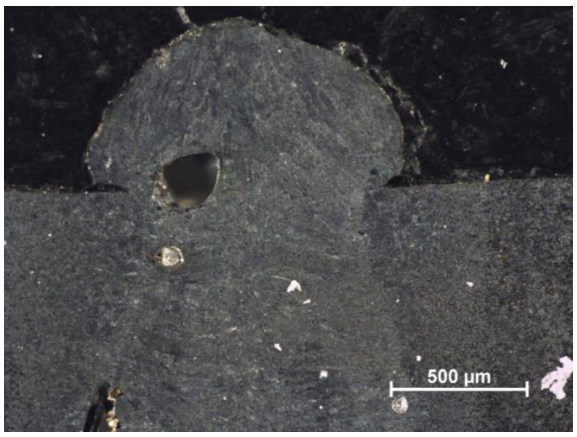

Fig. 9. *Sample 1*

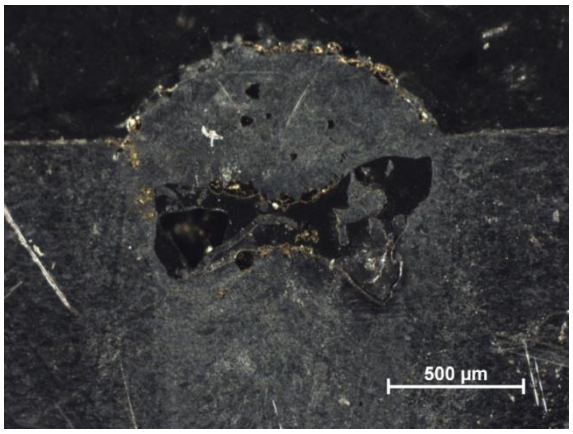

Fig. 10*. Sample 1.2*

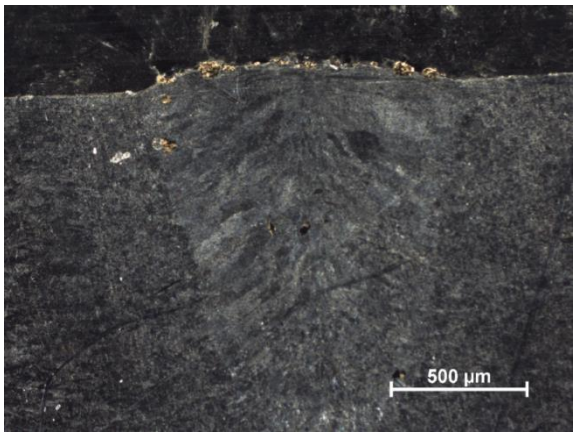

Fig. 11. *Sample 2*

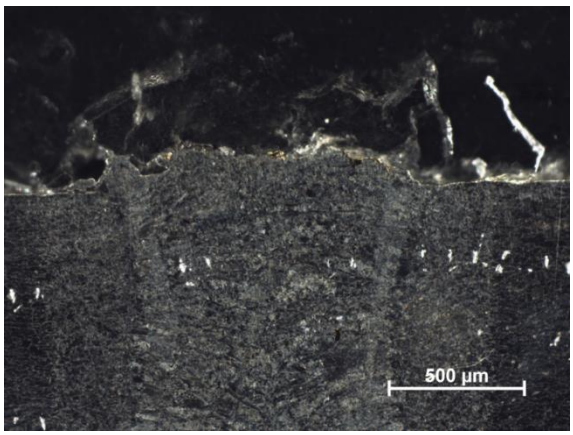

Fig. 12. *Sample 6*

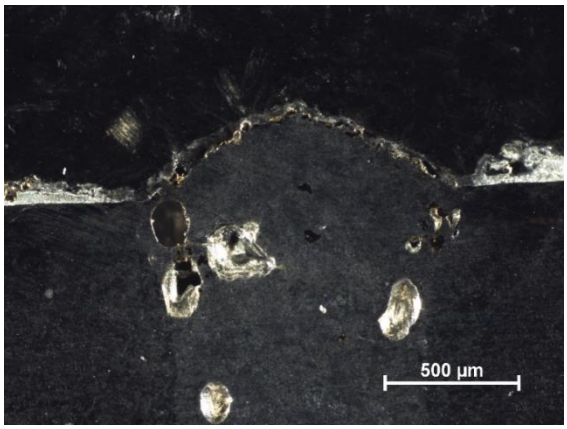

Fig. 13. *Sample 7*

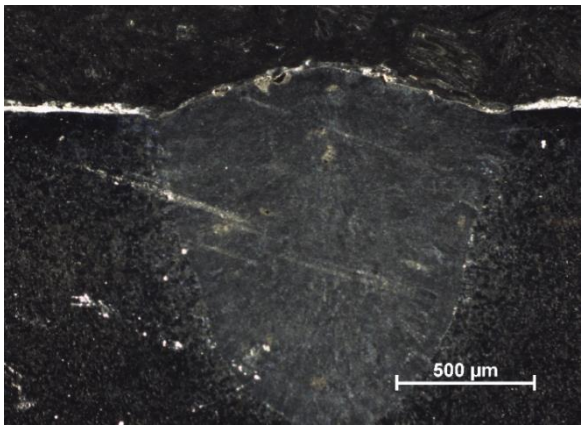

Fig. 14. *Sample 8*

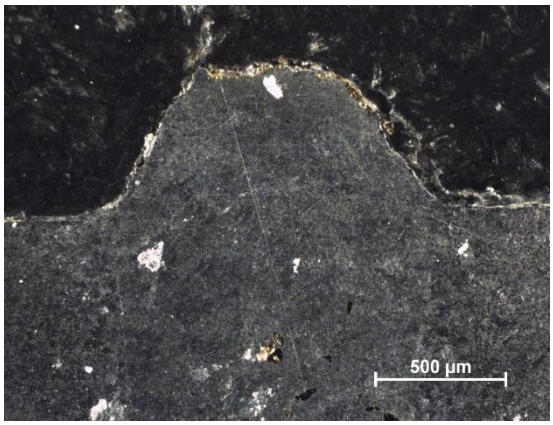

Fig. 15. *Sample 9*

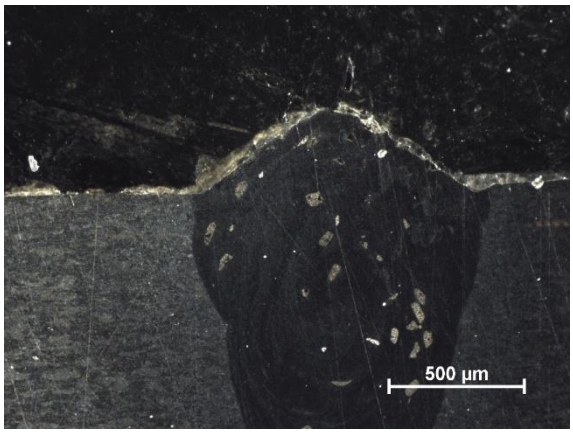

Fig. 16. *Sample 10*

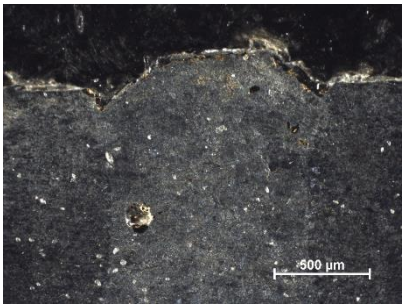

Fig. 17. *Sample 11*

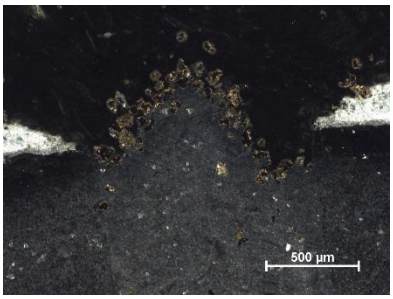

Fig. 18*. Sample 12*

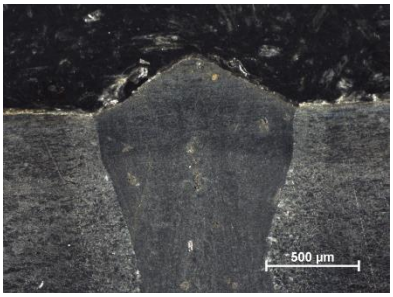

Fig. 19. *Sample 13*

Se puede observar que en prácticamente todas las muestras se forma la microcapa deseada, al menos parcialmente.

6. Conclusión

Tras estudiar las distintas muestras, se puede llegar a las siguientes conclusiones:

- El aumento de flujo de gas es negativo para la formación de la microcapa. Para aumentar la cantidad de polvo, es recomendable aumentar la velocidad de rotación de la mesa de alimentación.

- No hay efectos visibles en el cambio de material base ni de material de polvo. Esto último es probablemente debido a la semejanza entre las propiedades del TiN y el TiC.

- Con bajas velocidades de láser, el polvo aparece más fundido, lo cual es positivo para las propiedades de la superficie. Por otro lado, la velocidad del láser en el rango estudiado no parece tener efectos notorios sobre la cantidad de polvo presente.

- A más distancia entre la boquilla y el ojo de cerradura, menos polvo es depositado, debido al enfriamiento del material.

- El parámetro que más ha afectado al resultado es el lado en el que se coloca la boquilla. En la posición frontal, aumenta la cantidad de polvo presente en la sección transversal, debido a la mayor rapidez de llegada del polvo a la superficie.

Bibliografía

1. *Impact of process parameters on particle distribution and wear resistance during laser deep alloying processes.* **Volpp, Jörg; Zingraf, Alexander; Vollertsen, Frank. 2015.**

2. *Powder particle attacthment mechanism onto liquid material.* **Volpp, J.; Prassad, H.S.; Riede, M.; Brueckner, F.; Kaplan, A.F.H. 2018.**

3. *Particle property impact on its distribution during laser deep alloying processes.* **Volpp, J.; Dietz, T.; Vollertsen, F. 2014.**

4. *Direct laser sintering of metal powders: mechanism, kinetics and microstructural features.* **Smichi, A. 2006.**

5. *Behavior of heated powder particles on solid surfaces.* **Volpp, J.; Prasad, H.S.; Kaplan, A. 2018.**

6. *https://thermtest.com/materials-database#*

7. *Binding mechanisms in selective laser sintering and selective laser melting.* **Kruth, J.P.; Mercelis, P.; Van Vaerenbergh, J. 2005.**

8. *Direct Selective Laser Sintering of Hard Metal Powders: Experimental Study and Simulation.* **Wang, X.C.; Laoui, T.; Bonse,J.; Kruth, J.P.; Lauwers, B.; Froyen, L. 2002.**

9. *Homogeneity of TiC particles distribution during laser deep dispersing (2017 project).* **Bodén, F.; Cochrane, C.; Danielsson, C., García Pérez, J.; Sarentica, A.; Torres, H. 2017.**

10. *Thin layer of particles during deep penetration laser dispersing (2018 project).* **Blanc, A.; Da Silva, A.; Förster, G.; Kelly, S.; De la Llana Pablos, J.; Pastor, A.; Tedesi, M. 2018.**